Reducing Glucocorticoid Burden in Lupus with Omega-3 Fatty Acids: Docosahexaenoic Acid Augments Prednisone Efficacy in Maintaining Cyclophosphamide-Induced Remission of Preclinical Lupus Nephritis

Ashley N. Anderson[1], Olivia F. McDonald[1,2], Shayla-Rae S. Johnson[1], John J. Liddle[1], Vanessa Estrada[1,2], Jalen T. Jackson[1], Ryan P. Lewandowski[3], James G. Wagner[2,3], Jack R. Harkema[2,3,4], James J. Pestka[1,2,5.]

[1]Department of Microbiology, Genetics, and Immunology, Michigan State University, East Lansing, MI, United States; [2]Institute for Integrative Toxicology, Michigan State University, East Lansing, MI, United States; [3]Department of Pathobiology and Diagnostic Investigation, Michigan State University, East Lansing, MI, United States; [4]Department of Pharmacology and Toxicology, Michigan State University, East Lansing, MI, United States; [5]Department of Food Science and Human Nutrition, Michigan State University, East Lansing, MI, United States

Corresponding Author:

Dr. J.J. Pestka
Department of Microbiology, Genetics, and Immunology
Michigan State University
East Lansing, MI, United States
Email: pestka@msu.edu

Running Title: DHA Supplementation Augments Lupus Nephritis Remission

Keywords: NZBWF1 mouse, lupus nephritis, omega-3 fatty acid, prednisone, cyclophosphamide

Abstract

Background: Managing lupus nephritis (LN) remains challenging due to relapses after immunosuppressive induction and toxicity from long-term glucocorticoid (GC) maintenance therapy. Dietary omega-3 fatty acids prevent LN onset in preclinical models, but their role in maintaining remission post-induction remains unstudied.

Methods: The silica-accelerated LN (SALN) model using lupus-prone NZBWF1 mice was used to evaluate how docosahexaenoic acid (DHA), an omega-3 fatty acid, influenced LN remission durability after cyclophosphamide (CYC) induction, alone or with a moderate dose of prednisone (PDN). Mice received intranasal silica weekly from 8 to 11 weeks. After LN developed at 21 weeks, groups were injected weekly with CYC (human equivalent dose [HED]=31 mg/day) or vehicle (VEH) for 8 weeks, during which CYC groups also received control, DHA (HED=5 g/day), PDN (HED=9 mg/day), or DHA+PDN diets. Disease activity was monitored via proteinuria, autoantibodies, and survival. Six weeks post-CYC, multi-organ histopathology and immunohistochemistry were assessed.

Results: VEH-treated mice developed severe LN with early death. CYC slowed disease temporarily in control- and PDN-fed mice; relapses occurred after cessation. DHA or DHA+PDN increased tissue omega-3 levels and prolonged remission. PDN and DHA monotherapies and co-therapy improved survival, but DHA+PDN was most effective at sustaining remission as reflected by reduced histopathologic markers of lupus severity in the kidney, spleen, lung, and brain.

Conclusion: DHA+PDN optimally maintained LN remission after CYC, supporting omega-3 supplementation as a potential GC-sparing strategy to improve immunosuppressive therapy and prevent relapses.

Highlights

- Frequent post-immunosuppressive treatment flares and the toxicity from long-term maintenance therapy with glucocorticoids (GCs) limit effective management of lupus nephritis (LN).
- The silica-accelerated lupus nephritis (SALN) model in NZBWF1 mice mimics the gene–environment interactions of human systemic lupus erythematosus (SLE) and LN, enabling synchronized and efficient preclinical studies of drug and nutritional interventions.
- Short-term immunosuppressive therapy with cyclophosphamide (CYC) induces temporary remission of LN and extrarenal inflammation and autoimmunity in SALN mice, which can be extended through monotherapy with either dietary supplementation with omega-3 docosahexaenoic acid (DHA) or a moderate dose of the GC prednisone (PDN).
- Combined maintenance therapy with DHA and PDN proved more effective than monotherapy in enhancing the durability of post-CYC LN remission and in reducing extrarenal inflammation and autoimmunity in the lung, spleen, and brain.
- These preclinical findings show that dietary supplementation with omega-3s such as DHA may offer a safe, affordable, GC-sparing adjunctive option for managing LN and SLE.

Introduction

Systemic lupus erythematosus (SLE) is a severe, multifactorial autoimmune disease that causes immune-mediated damage across multiple organs, including the skin, spleen, lungs, brain, and kidneys [1-4]. Its onset and progression are driven by complex gene–environment interactions and characterized by recurrent flares that substantially increase morbidity and the risk of irreversible organ damage. Lupus nephritis (LN) is a major complication that can progress to end-stage renal disease when inadequately controlled [1,4,5].

Conventional therapy for advanced proliferative LN (Class III or higher) typically follows a two-phase paradigm to quell renal inflammation, suppress autoimmunity, and promote durable remission [6]. The induction phase uses potent immunosuppressants such as cyclophosphamide (CYC) to achieve LN remission, followed by a maintenance phase to sustain remission and limit cumulative damage, using tapered doses of glucocorticoids (GCs) like prednisone (PDN) together with other drugs, such as mycophenolate mofetil [7,8]. Although these regimens are effective, GCs have myriad adverse effects—including serious infections, fatigue, metabolic and cardiovascular complications, type 2 diabetes, bone loss, reproductive and hepatic toxicity, and bone marrow suppression—that pose ongoing challenges in selecting drugs, determining treatment duration, and designing tapering strategies. Importantly, prematurely reducing or stopping maintenance therapy significantly increases the risk of relapse and flaring [9]. Recent advances in biologic and targeted therapies have expanded the LN armamentarium and can theoretically reduce GC exposure [6], yet their high cost and restricted availability remain significant barriers for the ever-growing population of patients without adequate insurance coverage [10].

There is increasing recognition that dietary modulation has value as a complementary strategy for

83 treating persistent inflammatory and autoimmune diseases, an emphasis reflected in initiatives such
84 as the NIH Strategic Blueprint on Precision Nutrition and the NIH-Wide Strategic Plan for
85 Autoimmune Disease Research [11,12]. Consistent with this recognition, many clinicians are
86 adopting dietary counseling into routine SLE care [13], and there is particular interest in precision
87 nutrition approaches that target the tissue lipidome by increasing consumption of omega-3
88 polyunsaturated fatty acids (PUFAs) [14-16]. Western dietary patterns, typically enriched in omega-
89 6 PUFAs such as linoleic acid (LA) from seed oils and arachidonic acid (ARA), formed by LA
90 elongation and found in animal fat, are associated with worsening of chronic inflammatory states
91 driven by ARA-derived metabolites [17]. In contrast, diets or supplements rich in marine-derived
92 omega-3 PUFAs—especially docosahexaenoic acid (DHA) and eicosapentaenoic acid (EPA),
93 sourced from microalgae, krill, or cold-water fish oils—can attenuate inflammatory responses and
94 promote their resolution [18].

95 A well-established literature links DHA and EPA intake of 1 to 5 g/day to favorable changes in
96 cardiovascular risk biomarkers and outcomes, as well as clinical improvement in inflammatory
97 rheumatologic conditions [19-23]. Regulatory investigations confirm that combined EPA+DHA
98 supplementation up to 5 g/day is safe for adults [24]. This dosage costs approximately $2/day when
99 purchased over the counter as a stable, high-quality supplement [25]. Mechanistically, omega-3s are
100 rapidly incorporated into immune cell membranes and act by i) altering membrane fluidity and lipid
101 raft organization to modulate receptor clustering and downstream signaling, ii) dampening
102 activation of proinflammatory transcription factors such as NF-κB while activating others with anti-
103 inflammatory actions like PPAR-γ, iii) reducing proinflammatory gene expression and cytokine
104 production, iv) suppressing production of inflammatory ARA-derived leukotrienes, prostaglandins,
105 and thromboxanes by competitive inhibition, and v) serving as substrates for specialized pro-

106 resolving mediators that drive active resolution of inflammation and restoration of tissue
107 homeostasis [15,18,26]. Remarkably, many of these molecular targets overlap with or complement
108 those of GCs [27], offering promise of safe adjunctive omega-3 supplementation to reduce flare
109 frequency and slow kidney damage in individuals with lupus.

110 Preclinical investigations in lupus-prone mouse strains over four decades have consistently shown
111 that omega-3-enriched diets suppress or delay autoimmune responses, reduce the onset and
112 progression of LN, and improve survival rates [28-53]. In contrast, diets high in saturated fats,
113 monounsaturated fats, and omega-6s, typical of ultraprocessed foods, have been linked to increased
114 autoimmunity and kidney damage. Building upon this base, our lab has developed an efficient gene–
115 environment interaction model in autoimmune-prone NZBWF1 mice, in which short-term, repeated
116 intranasal instillations of crystalline silica ($cSiO_2$), a well-known environmental trigger of lupus,
117 accelerate systemic autoimmunity and LN by approximately three months, providing a highly
118 reproducible silica-accelerated LN (SALN) platform [54,55]. Within this model, oral
119 supplementation with microalgal oil–derived DHA at human equivalent doses (HEDs) of 2 to 5
120 g/day provides broad dose-dependent protection, including: i) suppression of inflammatory, type I
121 interferon, and autoimmune gene networks in the lung, ii) reduction of B- and T-cell infiltration and
122 ectopic lymphoid structure (ELS) formation, iii) lowering of pulmonary and systemic autoantibody
123 (AAb) titers, iv) prevention of glomerulonephritis, and v) prolonging survival [26,56-63].
124 Collectively, these studies position DHA supplementation as a suitable adjunctive strategy for
125 reducing GC use during LN treatment.

126 The SALN model has been further leveraged to assess the preventive effectiveness of the PDN,
127 demonstrating that oral pretreatment with a medium PDN dose (14 mg/day HED) substantially
128 reduced $cSiO_2$-induced pulmonary ELS formation, AAb production, and inflammatory and

129 autoimmune gene expression in the lung and kidney. This dose also reduced splenomegaly and the
130 severity of glomerulonephritis [64]. In contrast, low-dose PDN (5 mg/day HED) did not improve
131 autoimmune symptoms, whereas a high-dose PDN (46 mg/day HED) caused severe GC-associated
132 toxicity, leading to early cohort termination. Significantly, even at the effective medium dose, PDN
133 caused muscle wasting and did not improve survival. This indicates a discordance between
134 histopathologic improvements and death rates in SALN and confirms the narrow therapeutic
135 window of long-term GC therapy [64]. Furthermore, these observations suggest that, within the
136 constraints of the SALN model, DHA offers a more favorable balance between preventive
137 effectiveness and tolerability than PDN.

138 Although a substantial amount of preclinical data supports the use of omega-3s in lupus, including
139 research with DHA in SALN, these studies have primarily focused on prevention rather than
140 treatment of established disease. This limits their relevance for patients with SLE who often present
141 with active LN that requires remission induction. To address this gap, the SALN model was used
142 here to assess whether adjunctive DHA supplementation can maintain LN remission after
143 immunosuppressive induction with CYC, when administered either alone or combined with a
144 moderate, clinically relevant dose of PDN. We show for the first time preclinical evidence that
145 adjunctive DHA improves the efficacy of PDN, prolonging remission of both LN and extrarenal
146 lupus pathogenesis. Accordingly, safe, inexpensive omega-3 supplementation might serve as a GC-
147 sparing strategy to improve long-term disease management and reduce treatment-related toxicity in
148 LN and SLE.

149 Materials and Methods

150 Animals

151 All experimental protocols were reviewed and approved by the Institutional Animal Care and Use
152 Committee (IACUC) at Michigan State University in accordance with the NIH guidelines (AUF
153 #PROTO202400258). Female 7-week-old lupus-prone NZBWF1 mice were obtained from the
154 Jackson Laboratory (#100008, Bar Harbor, ME), randomly assigned four per cage with free access
155 to food and water, and kept at a consistent temperature (20–24°C) and humidity (30–70%) with a
156 12-hour light/dark cycle.

157 **Diets**

158 Diet formulations were based on the nutritionally balanced semi-purified American Institute of
159 Nutrition (AIN)-93G rodent diet containing 70 g soybean oil per kg of diet (AIN-93G rodent diet
160 #110700, Dyets Inc., Bethlehem, PA) [65]. Four experimental diets were used in the study (Table
161 1). The (i) basal control diet (CON) was made by replacing the 70 g/kg soybean oil with 60 g/kg of
162 high-oleic safflower oil (AVO high-oleic safflower oil, American Vegetable Oils, Inc., Commerce,
163 CA) and 10 g/kg of corn oil (Mazola Corn Oil, ACH Food Companies, Inc., Oakbrook Terrace, IL)
164 to supply essential fatty acids. For the (ii) DHA diet, 25 g/kg of high-oleic safflower oil was
165 substituted in the basal CON diet with 25 g/kg of microalgal oil containing 40% DHA (DHASCO,
166 DSM Nutritional Products, Columbia, MD), as described earlier [56,57]. This diet contained 10 g/kg
167 DHA, modeling human DHA intake of 5 g per day on a caloric basis (Table 1). For a patient, this
168 would be roughly equivalent to taking i) five triple-strength over-the-counter fish oil capsules daily,
169 each containing approximately 1 g of omega-3 fatty acids or ii) five prescription-grade omega-3
170 capsules used to treat hypertriglyceridemia. For the (iii) PDN diet and the (iv) combined DHA+PDN
171 diet, PDN was dissolved in a small amount of 100% (v/v) ethanol and added to both the basal CON
172 and DHA diets at 10 mg/kg, as previously described [64]. This dietary level corresponds to an HED
173 of 9.4 mg/day (Table 2) and was designated as "moderate" because it falls within the lower end of

174 the medium dose range (7.5 to 30 mg/d) used in GC treatment of rheumatic diseases [66].

175 **Crystalline silica ($cSiO_2$)**

176 $cSiO_2$ (Min-U-Sil-5, 1.5–2.0 μm average particle size, U.S. Silica, Katy, TX) was acid-washed in
177 1 M HCl at 100°C for 1 hour to remove surface contaminants that could obscure surface activity.
178 The $cSiO_2$ was then rinsed three times with sterile water and dried in an oven at 200°C to eliminate
179 water, endotoxins, and microbial contaminants. On each day of $cSiO_2$ instillation, a working stock
180 suspension of 40 mg/ml in Dulbecco's phosphate-buffered saline (DPBS) was prepared, then
181 sonicated for 1 minute using the Q125 Qsonica sonicator (Qsonica LLC, Newtown, CT) set to 2
182 minutes with pulses of 5 seconds on and 5 seconds off at 35% amplitude. After sonication, the
183 suspension was inverted and vortexed continuously during instillations to prevent $cSiO_2$ settling.

184 **Experimental design**

185 The experimental study design is depicted in Figure 1. NZBWF1 mice (7 weeks old) were started
186 on the CON diet, and one week later, they were anesthetized with 4% isoflurane and intranasally
187 instilled with 1.0 mg of $cSiO_2$ in 25 μl of DPBS once a week for 4 weeks [54]. The total $cSiO_2$ dose
188 (4 mg) approximately equals half of a human lifetime exposure according to guidelines set by the
189 Occupational Safety and Health Administration (OSHA)[67]. At 20 weeks of age, $cSiO_2$-treated
190 mice were divided into weight-based quartiles, with 1 mouse from each quartile housed together,
191 totaling 4 mice per cage. This grouping ensured balanced experimental conditions, reducing
192 confounding effects from body weight differences. At 21 weeks, when $cSiO_2$-treated mice exhibit
193 proteinuria, cages were split into five treatment groups: (i) weekly DPBS vehicle (VEH)
194 intraperitoneal (IP) injections with the CON diet ($cSiO_2$/VEH/CON), (ii) weekly CYC IP injections
195 at 35 mg/kg body weight (bw) with the CON diet ($cSiO_2$/CYC/CON), (iii) weekly CYC IP injections

196 with a DHA diet ($cSiO_2$/CYC/DHA), (iv) weekly CYC IP injections with a PDN diet
197 ($cSiO_2$/CYC/PDN), and (v) weekly CYC IP injections with a DHA+PDN diet
198 ($cSiO_2$/CYC/DHA+PDN) (Figure 1). To reduce lipid oxidation products, diets were prepared every
199 two weeks, stored at -20°C until used, and provided fresh to the mice daily. Injections with VEH or
200 CYC ceased after 8 weeks, but mice remained on their respective maintenance diets for the
201 remainder of the study. Urine was collected weekly and tested for protein using reagent dipsticks
202 (Siemens Uristix 4, Malvern, PA). Plasma samples were collected biweekly, starting at 27 weeks of
203 age, for blood urea nitrogen (BUN) and AAb analyses. Mice were monitored daily for clinical signs
204 of moribundity (Supplementary Table 2) during feedings, and their body weights were recorded
205 weekly. Any mice meeting moribund criteria were immediately euthanized and necropsied. The
206 study concluded at age 35 weeks with a full necropsy of all remaining animals.

207 **Necropsy and tissue selection for light microscopy**

208 Mice were anesthetized at the end of the study with IP injections at 250 mg/kg bw of sodium
209 pentobarbital. A midline laparotomy was performed, and approximately 0.8 ml of blood was drawn
210 from the inferior vena cava and collected in heparinized tubes (MiniCollect Capillary Blood
211 Collection Tube #450477, Greiner Bio-One, Monroe, NC). Animals were euthanized by
212 exsanguination through the inferior vena cava. After death, the trachea was exposed, cannulated,
213 and the heart and lungs were excised en bloc. A volume of 0.7 ml sterile saline was instilled via the
214 tracheal cannula and then withdrawn to recover bronchoalveolar lavage fluid (BALF). A second
215 intratracheal saline lavage was performed, and the collected BALF was combined with the first
216 sample. Organs selected for light microscopy and digital image analysis were harvested at necropsy
217 and fixed in 10% neutral buffered formalin for at least 48 hours. The left kidney, spleen, and brain
218 were fixed by immersion, while the left lung lobe was fixed by fluid inflation via the trachea at 30

219 cm gravitational pressure as previously described [57].

220 After fixation, cross-sectional (transverse/coronal) tissue blocks were cut from the left kidney (1-2
221 blocks covering the entire organ), left lung lobe (4 blocks covering the entire lobe), spleen (2 mid-
222 blocks from the body of the organ), and brain (1 block with hippocampus, at the level of the inner
223 ear). Tissue blocks were paraffin-embedded and sectioned at 5 microns. Tissue sections were stained
224 histochemically with Hematoxylin and Eosin (H&E, all organs) or Periodic Acid Schiff (PAS,
225 kidney) and immunohistochemically stained for $CD3^+$ and $CD45R^+$ T and B lymphoid cells,
226 respectively (lung and kidney), IBA-1^+ monocytes/macrophages (lung and kidney), and IBA-1^+
227 microglia in the hippocampus (brain). Details for immunohistochemistry and specific antibodies are
228 provided in the Supplemental Materials.

229 **Quantitative and semi-quantitative image analysis of histopathology**

230 Digital images of histological sections were obtained with an Olympus VS200 slide scanner with
231 ASW software (V.3.2.1) at 20x magnification (Evident Scientific, Waltham, MA). Digitally scanned
232 images were viewed with Olympus OlyVIA software (V.2.8) and whole-slide image analyses were
233 conducted using QuPath image analysis software (V.0.5.1) [68]. Regions of interest (ROIs) were
234 annotated prior to each quantitative analysis (Lung, whole lung lobe sections; Kidney, renal cortex
235 in sections). Abundance of immunohistochemical stains (density of IBA-1^+, $CD3^+$, $CD45R^+$) was
236 graphically expressed as the percent of ROI area. Thresholds were created to model staining
237 positivity per tissue type. Identical settings per stain were used to assess positivity among
238 experimental groups.

239 Semi-quantitative image analysis of histopathologic severity was conducted for specific lupus-
240 related lesions: membranous glomerulonephritis, renal tubular regeneration, accumulated protein in

241 renal tubular lumens, ectopic lymphoid structures (ELS, $CD3^+$ T cells and $CD45R^+$ B cells) in the
242 kidney, white pulp hyperplasia in the spleen, and microgliosis in the hippocampus of the brain (IBA-
243 1^+ microglia). A board-certified veterinary pathologist (JRH) examined all digitally scanned images
244 of routine H&E- and immunohistochemically stained tissue sections for $cSiO_2$-triggered lupus
245 histopathology using unbiased blinded assessment (no previous knowledge of individual animal
246 exposure or treatment). Lesion severity scores were recorded in a manner that is consistent with
247 state-of-the-art guidelines for semi-quantitative pathology assessment [69]. Criteria for ordinal
248 scoring were defined by percent of total tissue affected: 0 (no lesions) = 0% of total tissue; 1
249 (minimal) = less than 5%; 2 (mild) = 6 to 10%; 3 (moderate) = 11 to 50%; 4 (marked) = 51 to 75%;
250 5 (severe) = greater than 76%.

251 **Red blood cell (RBC) fatty acid analysis**

252 RBC fatty acid composition was analyzed using gas chromatography (GC) with flame ionization
253 detection by OmegaQuant Analytics (Sioux Falls, SD) as described previously [63]. Briefly, after
254 isolating RBCs from heparinized blood, fatty acid methyl esters (FAMEs) were prepared by heating
255 the RBCs with 14% boron trifluoride-ethanol and hexane at 100°C for 10 minutes. The FAMEs
256 were then extracted with hexane and analyzed on a Shimadzu GC-2010 chromatograph equipped
257 with an SP-2560 100-m capillary column. Fatty acids were identified by comparison to a
258 commercial standard (GLC OQ-A, NuCheck Prep). A total of 24 fatty acids were quantified and
259 expressed as a percentage of the total identified fatty acids, including saturated, monounsaturated
260 (cis and trans), and polyunsaturated (omega-3 and omega-6) species.

261 **Autoantibody (AAb) measurement**

262 IgG AAbs targeting silica-killed cell (SKC) autoantigens (AAgs) and dsDNA were measured using

263 an indirect ELISA based on a previously described method [70]. To prepare SKC AAgs, fetal liver-
264 derived alveolar-like macrophages (FLAMs) from lupus-prone NZBWF1 mice were exposed to 50
265 μg/ml $cSiO_2$ for 20 hours to induce cell death. The supernatant was then collected and stored at -
266 20°C until use. Poly-L-lysine-coated 96-well microplates were incubated with a blocking buffer
267 (PBS, 2% [w/v] BSA, 0.05% [v/v] Tween 20), then coated with 50 μl per well of either SKC AAg
268 diluted 1:20 or calf thymus dsDNA diluted to 2.5 μg/ml, both prepared in ELISA buffer (PBS, 0.1%
269 [w/v] BSA, 0.05% [v/v] Tween 20). Next, diluted BALF (1:1,000) or plasma (1:5,000 and 1:10,000)
270 was added to separate wells. A standard curve was generated using two-fold serial dilutions of a
271 mouse anti-dsDNA antibody, with the highest concentration assigned a value of 2,000 arbitrary units
272 (U). Bound AAbs were detected using HRP-conjugated goat anti-mouse IgG Fc antibody and K-
273 Blue® Advanced Plus TMB Substrate, with absorbance measured at 650 nm.

274 **Blood urea nitrogen (BUN) analysis**

275 BUN was measured using the Ray Biotech Urea Nitrogen Detection Assay Kit (MA-BUN-5) per
276 manufacturer's directions. Briefly, plasma samples were diluted 1:20, loaded onto a microplate, and
277 then incubated with an enzyme solution of urease and NADH. After a brief shaking of the plate,
278 absorbance was measured (340 nm) twice, with one minute between readings. The difference in
279 absorbance between the two readings correlates with BUN concentration. BUN levels were
280 determined using a standard curve.

281 **Bronchoalveolar lavage fluid (BALF) cell quantitation and identification**

282 Total cells in BALF were counted using a hemocytometer. Cytological slides were prepared by
283 centrifuging 150 μl of BALF for 10 minutes at 40 × *g*, air-drying, and staining with the Easy III Step
284 Stain Kit (#ES902, Azer Scientific, Morgantown, PA). At least 150 cells were counted and

285 differentially identified as monocytes/macrophages, lymphocytes, or neutrophils based on
286 morphological criteria.

287 **Statistical analysis**

288 All treatment groups began with 8 mice. All statistical analyses were conducted using GraphPad
289 Prism 10 (V.10.6.1, Dotmatics, Boston, MA), with a p-value < 0.05 considered significant.
290 Parametric two-tailed t tests (with and without Welch's correction) or nonparametric Mann-Whitney
291 tests were used to compare the continuous quantitative data and the ordinal histopathological
292 severity scores between the $cSiO_2$/VEH/CON (negative control) and $cSiO_2$/CYC/CON (positive
293 control) groups, respectively. When comparing the continuous quantitative data across the treatment
294 groups ($cSiO_2$/CYC/CON, $cSiO_2$/CYC/DHA, $cSiO_2$/CYC/PDN, $cSiO_2$/CYC/DHA+PDN), several
295 statistical tests were performed: (i) parametric one-way ANOVAs along with the Brown-Forsythe
296 test of equal variances, (ii) parametric Brown-Forsythe and Welch one-way ANOVAs, and (iii)
297 Dunnett's and Tukey's multiple comparisons tests. When comparing the semi-quantitative ordinal
298 severity score data of the treatment groups, the nonparametric Kruskal-Wallis and Dunn's multiple
299 comparisons tests were used.

300

301 **Results**

302 **Dietary DHA remodels RBC membrane fatty acid composition**

303 The dietary DHA intervention was confirmed to induce systemic lipidomic changes by assessing
304 the fatty acid composition of RBC phospholipids, which serves as a biomarker of overall tissue lipid
305 status (Figure 2; Table 3) [71]. Mice receiving isocaloric DHA-supplemented diets

306 ($cSiO_2$/CYC/DHA and $cSiO_2$/CYC/DHA+PDN groups) exhibited significant increases (up to 10- to
307 12-fold) in DHA and other omega-3 fatty acids, including EPA and omega-3 docosapentaenoic acid
308 (DPA). This increase was accompanied by a marked decrease in total omega-6 fatty acids (up to 50
309 to 70%), such as ARA, omega-6 DPA, and docosatetraenoic acid, with the exception of linoleic acid
310 (LA), which was significantly elevated. Notably, RBCs from mice treated with DHA and PDN
311 contained higher levels of DHA, EPA, and total omega-3s than those from mice receiving DHA
312 alone, along with lower levels of ARA and total omega-6 fatty acids. In contrast, PDN treatment
313 alone did not alter fatty acid profiles, indicating that the observed lipidomic changes were
314 specifically attributable to dietary DHA intake.

315 **DHA and PDN co-therapy after CYC induction prevents proteinuria relapse and death.**

316 Consistent with previous studies in NZBWF1 mice [54,56,61], weekly intranasal $cSiO_2$ instillations
317 for 4 weeks in control-fed mice resulted in two main clinical outcomes: proteinuria (Figures 3A-C)
318 and shortened lifespan, with a median survival of 29.5 weeks (Figure 3D). CYC treatment alone
319 reduced proteinuria, but relapses happened after stopping, as evidenced by increased proteinuria at
320 week 33 (Figure 3A), and increased median survival to 35 weeks (Figure 3D). Maintenance
321 therapies with either DHA or DHA+PDN delayed relapse, whereas PDN alone did not. The mean
322 percentage of proteinuric mice (Figure 3B) and mean proteinuria levels (Figure 3C) from weeks 21
323 to 35 were significantly lower in the CYC/DHA and CYC/DHA+PDN groups than in the CYC-only
324 or CYC/PDN groups. Maintenance treatments also conferred a survival advantage, with median
325 survival times for both monotherapies and combination therapy exceeding 35 weeks (Figure 3D).

326 **Combining DHA and PDN maintenance therapy preserves renal structure and reduces**
327 **macrophage infiltration.**

328 Kidneys from $cSiO_2$/VEH/CON mice exhibited severe membranous glomerular nephritis,
329 characterized by glomerular enlargement, extensive accumulation of PAS^+ glomerular membranous
330 tissue, and proteinaceous casts in the renal tubules (Figure 4B). These features were absent in age-
331 equivalent naïve mice from a prior study [61] and used here as a standard reference control (Figure
332 4A). Conversely, CYC treatment reduced glomerulonephritis (Figure 4C), and this improvement
333 was further enhanced by DHA (Figure 4D) and PDN (Figure 4E). The group receiving combination
334 therapy ($cSiO_2$/CYC/DHA+PDN) was the most protected from these pathological changes and
335 displayed nearly normal renal structure (Figure 4F). Semi-quantitative scoring confirmed that the
336 combination therapy decreased the LN severity score ($p<0.01$) (Figure 4G), tubular protein score
337 ($p=0.11$) (Figure 4H), and tubular regeneration score ($p<0.05$) (Figure 4I) compared to CYC
338 treatment alone.

339 IHC staining for IBA-1, a well-known marker for recruited inflammatory monocytes/macrophages
340 [72], showed that, consistent with glomerulonephritis, $cSiO_2$ exposure caused significant infiltration
341 of monocytes/macrophages into interstitial spaces surrounding renal tubules and glomeruli, in ELS,
342 and some glomeruli (Figures 5A, 5B). While modestly reduced by CYC with DHA or PDN
343 monotherapies (Figures 5D, 5E, 5G), IBA-1^+ monocyte/macrophage infiltration was most robustly
344 reduced by co-therapy with CYC/DHA+PDN (Figures 5F, 5G). Accordingly, DHA+PDN co-
345 treatment was the most effective of the three maintenance therapies in reducing local renal
346 inflammation and preserving kidney structure.

347

348 **DHA and PDN co-therapy prevents the formation of renal ELS**

349 A key pathogenic feature of progressive LN is the formation of renal ELS [73-75]. The renal cortices

350 of $cSiO_2$-triggered mice that did not receive treatment contained large, organized ELS composed of
351 co-localized aggregations of IBA-1$^+$ macrophages, CD3$^+$ T cells, and CD45R$^+$ B cells (Figure 6A,
352 C, E, G). Maintenance therapy with CYC/DHA+PDN effectively prevented this process, as kidneys
353 from this group were mostly free of dense lymphoid cell aggregate infiltrates and lacked organized
354 ELS architecture (Figure 6B, D, F, H). The kidney ELS score was lower ($p<0.05$) in the
355 CYC/DHA+PDN co-therapy group compared to the CYC-only and CYC/DHA groups, while the
356 PDN monotherapy was less effective (Figure 6I).

357

358 **Protective effects of DHA and PDN monotherapy and co-therapy extend to the lungs.**

359 In NZBWF1 mice, age-related pulmonary perivascular and peribronchiolar lymphoid hyperplasia
360 spontaneously occurs at 8 to 12 months of age, during which polymorphic lymphoid infiltrates,
361 evocative of ELS, become dominated by CD4$^+$ T cells, while B cells and antigen-presenting cells
362 segregate into a peripheral cuff surrounding the T cell–rich area [76,77]. This occurs much earlier
363 in the SALN model, where the lung is the hub for early cellular events that promote $cSiO_2$-induced
364 autoimmunity and the progression of lupus [78]. Cellular analysis of BALF demonstrated that DHA
365 and PDN monotherapies, as well as combination therapy with CYC, reduced total inflammatory
366 cells, monocytes/macrophages, and lymphocytes compared to CYC alone (Figure 7A). Furthermore,
367 combined DHA+PDN treatment exhibited a modest trend toward reduced local production of IgG
368 autoantibodies against dsDNA and $cSiO_2$-killed cells (Figure 7B).

369 Histological examination of lung tissue showed that, as previously reported [54,55], strong
370 perivascular ELS appeared in $cSiO_2$-treated mice (Figures 8C, D) and were absent in naïve mice
371 (Figures 8A, B). Consistent with decreased cellularity in BALF, ELS were markedly reduced in the

372 lungs of the CYC/DHA+PDN group (Figures 8K, L), while effects of monotherapies were more
373 modest (Figures 8G-J). Semi-quantitative scoring confirmed that the DHA+PDN combination
374 maintenance therapy significantly lowered lung ELS scores ($p<0.001$ and $p<0.05$) compared to
375 CYC-only and CYC/PDN, respectively (Figure 9A) and modestly decreased the percentage of $CD3^+$
376 T cells (Figure 9C), while both CYC/PDN and CYC/DHA+PDN significantly decreased the
377 percentage of $CD45R^+$ B cells ($p<0.05$ and $p<0.01$) compared to CYC-only, respectively (Figure
378 9D).

379

380 **DHA+PDN co-therapy suppresses $cSiO_2$-induced splenomegaly and systemic AAbs**

381 The spleen is another potential source of systemic AAbs in NZBWF1 mice [79], and splenomegaly,
382 a key feature of spontaneous lupus progression in these mice, is accelerated by $cSiO_2$ treatment [64].
383 Therefore, to evaluate the effects of treatments on systemic autoimmunity, we compared spleen
384 architecture and plasma AAbs across the experimental groups. $cSiO_2$ caused significant white pulp
385 hyperplasia in mice (Figures 10B, H), which was not evident in age-equivalent naïve NZBWF1 mice
386 (Figure 10A). Lymphoid cell hyperplasia was not substantially affected by CYC alone (Figure 10C)
387 or by CYC in combination with DHA or PDN alone (Figures 10D, E); however, it was suppressed
388 in CYC-treated mice that received DHA+PDN (Figure 10F). For other indicators of splenomegaly,
389 spleen weight and area, DHA and PDN monotherapies showed modest reductions, while
390 DHA+PDN co-therapy showed marked decreases (Figures 10G, H, and I). Treatment effects on the
391 spleen were consistent with plasma dsDNA and SKC AAb levels (Figure 10J). After stopping CYC,
392 plasma IgG AAbs against dsDNA and SKC began to rise again within 4 to 6 weeks post-CYC
393 treatment in the CYC-only and CYC/DHA groups. This increase was consistently suppressed in

394 groups receiving PDN, either alone or with DHA. Overall, DHA potentiates PDN suppression of
395 splenomegaly and systemic AAb formation resulting from $cSiO_2$ instillation.

396

397 **DHA and PDN co-therapy attenuates microglial cell activation in the brain**

398 NZBWF1 mice have been used in neuropsychiatric lupus (NPSLE) research, with IBA-1 positivity
399 in the brain (i.e., microgliosis) and microglial activation serving as markers of central nervous
400 system (CNS) inflammation [80-82]. In the hippocampus, $cSiO_2$/VEH/CON mice exhibited
401 pronounced microgliosis, characterized by increased density and altered shape of IBA-1^+ microglial
402 cells (Figures 11A, B). This neuroinflammatory state was diminished in mice that received CYC,
403 CYC/DHA, and CYC/PDN (Figures 11C, D, and E), and was maximally reduced in mice receiving
404 CYC/DHA+PDN co-therapy, which displayed a more resting microglial appearance (Figure 11F).
405 This was further reflected in markedly lower microgliosis scores for the DHA+PDN co-therapy
406 group, suggesting that the benefits of this combination extend to reduced CNS-related inflammation
407 (Figure 11G).

408

409 **Discussion**

410 LN remains difficult to manage, and there is a significant need for innovative strategies that sustain
411 long-term remission while enabling a meaningful reduction in GC doses. Observational SLE studies
412 have linked higher omega-3 intake and circulating DHA with diminished disease activity as
413 reflected in SLAQ scores and better patient-reported outcomes, including reduced pain and
414 improved sleep [83-85]; however, randomized controlled trials (RCTs) have yielded mixed results.

415 Akbar et al. [22] reported variable benefits across nine RCTs that differed in duration (10–
416 52 weeks), sample size (12–85 participants), and dosage (0.54–3.60 g EPA; 0.30–2.25 g DHA).
417 Several studies reported improvements in clinical or serologic markers [86-90], while others
418 observed only transient or no benefit [32,91-93]. A recent RCT using krill oil (4 g/day; 722 mg EPA,
419 384 mg DHA) showed positive effects in patients with high baseline disease activity (SLEDAI-
420 2K ≥ 9) [16]. Overall, although omega-3 RCTs suggest a potential for modest improvement in SLE
421 disease activity, small sample sizes, inconsistent dosing, varied populations, short follow-up
422 periods, limited assessment of long-term tissue FA incorporation, and suboptimal control of
423 confounding factors hinder clear interpretation. Therefore, the full extent of omega-3s' benefits for
424 individuals with SLE and LN, along with how they interact with standard treatments, remains
425 unclear.

426 Because omega-3 supplements are not patent-protected, large, highly optimized randomized
427 controlled trials used to evaluate new drugs are impractical, stressing the importance of rigorous
428 preclinical models to define their therapeutic potential in LN. In this context, the SALN model offers
429 a stringent, translationally relevant platform for evaluating remission-maintenance strategies after
430 immunosuppressive induction. Mechanistically, short-term, repeated $cSiO_2$ exposure in NZBWF1
431 mice combines an environmentally relevant trigger with genetic susceptibility. Inhaled particles are
432 initially phagocytosed by alveolar macrophages (AMs). This results in phagolysosome
433 destabilization, inflammasome activation, and AM death via pyroptosis and necrosis, and ultimately
434 the release of cytokines, chemokines, DAMPs, nuclear antigens, and $cSiO_2$ into the local
435 environment [78,94] (Figure 12). These events, together with the long pulmonary half-life of $cSiO_2$,
436 create a self-sustaining loop in which dying and activated AMs promote ELS formation in the lung,
437 enhance T- and B-cell recruitment and activation, and accelerate the production of pathogenic AAbs.

438 This process drives both pulmonary and systemic autoimmunity and results in severe, synchronized
439 glomerulonephritis (GN) that resembles key features of human SLE and LN [55,56]. Compared with
440 the spontaneous NZBWF1 model, SALN presents a condensed, synchronized multi-organ disease
441 course, with LN developing within 3 months after the final $cSiO_2$ exposure. This allows intervention
442 studies to be completed in 7 months, rather than 10 to 12 months in the conventional NZBWF1
443 model.

444 Previous investigations employing SALN have shown that either DHA or PDN monotherapy can
445 prevent LN onset [56-58,60-62,95], but these studies mainly focused on disease prevention. The
446 present study is innovative because it endeavors to bridge this translational gap by using SALN to
447 assess DHA as an adjunct therapy to prolong CYC-induced remission, both alone and in
448 combination with a modest, clinically relevant dose of PDN in established LN. We report for the
449 first time that dietary DHA administered post-LN onset during and after immunosuppressive
450 induction prompts significant remodeling of tissue membrane lipid composition. This change is
451 associated with enhanced clinical and histopathological outcomes (Figure 12). Incorporation of
452 DHA and other omega-3 fatty acids into phospholipids, along with a reciprocal depletion of omega-
453 6 species, most notably ARA, indicates robust reprogramming of tissue lipid pools. In mice given
454 DHA+PDN, increases in total omega-3 and decreases in omega-6 were enhanced by 33 percent and
455 19 percent, respectively, compared with mice fed DHA alone. In the kidney, DHA, particularly
456 when combined with PDN, prolonged CYC-induced remission by delaying proteinuric relapse and
457 maintaining renal structure. This was evidenced by reduced macrophage infiltration, diminished
458 tubular protein deposition, and prevention of ELS formation.

459 The benefits of DHA combined with PDN were observed beyond the kidney. In the lung, this
460 combination reduced perivascular inflammation, ectopic lymphoid aggregates, and local

461 autoantibody production. Systemically, it decreased splenomegaly and circulating autoantibodies.
462 In the brain, DHA+PDN reduced hippocampal microgliosis and improved neural tissue health,
463 indicating a wider impact on neuroinflammatory pathways in the CNS. Collectively, this evidence
464 indicates that DHA-rich nutrition, particularly when combined with PDN, exerts coordinated
465 immune-modulating effects across multiple organs, enhances the durability of LN remission, and
466 reduces extra-renal inflammation and tissue damage, thereby supporting its ability to augment SLE
467 outcomes more broadly. Thus, adjunctive DHA may enhance conventional two-phase
468 immunosuppressive therapy and is consistent with current rheumatology treatment approaches
469 focused on sustained remission with reduced GC exposure [9].

470 The organ-level effects observed here in SALN align with the well-known immunomodulatory
471 actions of omega-3 fatty acids. DHA and other omega-3s affect immune responses through
472 interrelated structural, transcriptional, and metabolic pathways [17,18,96,97]. Their incorporation
473 into membrane phospholipids alters lipid raft organization, increases membrane fluidity, and
474 interferes with receptor clustering required for effective signaling through TLRs, TNFR, and IL1R
475 [98]. At the transcriptional level, DHA suppresses NF-κB and activates PPARγ and NRF2,
476 diminishing oxidative stress and decreasing expression of proinflammatory mediators such as IL6
477 and iNOS [99,100]. Additionally, omega-3s inhibit ARA production from plant-derived LA [101]
478 and competitively inhibit the formation of inflammatory mediators from ARA, such as leukotrienes,
479 prostaglandins, and thromboxanes [96]. DHA also serves as a precursor for proresolving mediators
480 that promote efferocytosis, facilitating the clearance of apoptotic cells and supporting the resolution
481 of chronic inflammation [97]. The evidence presented here is further consistent with preventive
482 studies in NZBWF1 mice exposed to $cSiO_2$, where DHA elicits broad anti-inflammatory and
483 immunoregulatory actions in the lungs [63]. Following a single intranasal $cSiO_2$ challenge, control-

484 fed mice showed increased leukocyte influx, cytokine and chemokine levels, dead cell
485 accumulation, and higher AAbs in BALF. In contrast, DHA-enriched diets lessened these responses,
486 including IL1α, IL6, GM-CSF, CCL2, CCL3, and CXCL10, and lowered autoimmune-related gene
487 signatures linked to type I IFN signaling, TLR activation, and lymphocyte activation, with predicted
488 suppression of regulators like TNFα, IL1β, IFNAR, and IFNγ.

489 The tissue-specific effects of PDN in SALN observed here are in accord with the known
490 immunomodulatory actions of GCs. Treatment with PDN and other synthetic GCs rapidly controls
491 inflammation in SLE and related rheumatic conditions by activating the glucocorticoid receptor
492 (GR), which suppresses NF-κB/AP-1–driven inflammatory pathways in lymphoid and myeloid cells
493 and enhances anti-inflammatory genes like glucocorticoid-induced leucine zipper (GILZ) and dual
494 specificity phosphatase 1 (DUSP1) [102-104]. Non-genomic GR signaling further contributes by
495 inhibiting PLA2 and activating MAPK and cAMP pathways [102,104,105]. Additionally, GCs
496 modify lipid rafts by altering their lipid composition and physical properties, disrupting raft
497 formation in some immune cells while also recruiting GRs and related signaling complexes into
498 flotillin- or caveolin-rich raft regions, thereby affecting kinase signaling and gene regulation [106-
499 108]. Thus, the anti-inflammatory effects of DHA and PDN involve multiple parallel interconnected
500 mechanisms.

501 Using SALN, we previously found that pretreatment with a moderate PDN dose (14 mg/day HED),
502 taken orally via diet, significantly reduced $cSiO_2$-induced pulmonary ELS formation, AAb
503 production, and autoimmune gene expression in both the lung and kidney [64]. This treatment also
504 decreased splenomegaly and the severity of glomerulonephritis. Instead of reversing disease
505 signatures, this regimen reduced the magnitude and diversity of transcriptomic changes across
506 organs, showing a general suppression of autoimmune activation. Key adaptive immune modules—

507 including T-cell receptor signaling, antigen presentation, B-cell activation, and Fc-mediated effector
508 pathways—were particularly suppressed, especially in the lung. Overall, these prior findings show
509 that moderate-dose PDN provides widespread but incomplete transcriptional control over the $cSiO_2$-
510 induced autoimmune process, with innate and stress responses still partly active.

511 The PDN dose used in the present study was specifically chosen based on its narrow preventive
512 window in SALN: 14 mg/day HED reduces disease progression, 5 mg/day is ineffective, and
513 46 mg/day causes severe GC-related toxicity without providing a survival benefit [64]. This pattern
514 parallels clinical experience, in which high-dose GCs induce remission but carry significant
515 cumulative toxicity, and highlights that monotherapy suppresses inflammation without restoring
516 immune homeostasis [109]. Based on this prior study, herein we deliberately selected a suboptimal
517 intermediate dose (9.4 mg/day HED), positioned between previously ineffective and minimally
518 effective levels in SALN [64]. Clinically, this dose is near the lower end of moderate-dose GC
519 exposure: in a large SLE cohort, the mean daily PDN-equivalent dose during the first treatment year
520 was 19.4 mg, with about 60% of patients receiving ≥15 mg/day and only 17% maintained below
521 7.5 mg/day [110]. The 9.4 mg/day HED selected here represents a clinically significant exposure,
522 half of the dose usually employed during the first year of treatment, but still above the current treat-
523 to-target guidelines not to exceed 5 to 7.5 mg/day for SLE and LN maintenance.

524 Macrophages play a vital role in SLE development, driven by unresolved tissue inflammation,
525 defective removal of cellular debris, and persistent type I IFN signaling [111-113]. In a recent in
526 vitro study using a novel self-renewing AM model derived from embryonic NZBWF1 mouse liver,
527 we determined that DHA synergistically enhances the suppressive effects of low doses of the water-
528 soluble GC dexamethasone (DEX) on LPS-induced type 1 IFN-driven gene expression [27]. When
529 combined, subinhibitory levels of DHA and DEX led to over tenfold greater gene suppression than

530 either agent alone. This combination significantly reprogrammed inflammatory transcriptional
531 networks, decreasing activity in the NFκB, AP1, IRF, and STAT pathways while promoting
532 pathways associated with resolution and M2 polarization. These in vitro mechanistic insights align
533 with the in vivo SALN results discussed here, further supporting DHA as an adjunct therapy to GC
534 and highlighting its potential to enhance treatment outcomes by targeting critical pathogenic
535 pathways in SLE.

536 Interpretation of these data must consider several limitations. First, the relatively short experimental
537 duration limits conclusions about long-term disease progression and survival, and formal dose–
538 response relationships for both DHA and PDN—individually and together—are yet to be
539 systematically established. Second, the study was intentionally designed to focus on remission
540 maintenance, renal and extrarenal histopathology, and survival rather than a detailed mechanistic
541 analysis of how upstream signaling pathways are affected by DHA and PDN. Third, variations in
542 omega-3 types (DHA vs EPA) and bioavailability (ethyl esters, triglycerides, phospholipids) among
543 formulations on the market may additionally impact treatment effectiveness [16]. Finally, the
544 metabolic and immunological features of SALN may not fully parallel human SLE, so caution is
545 necessary when extrapolating to diverse patient populations. Therefore, to address these limitations,
546 future preclinical research using the SALN model should i) explicitly address dose–response
547 relationships over an extended time period, ii) compare various therapeutic formulations and
548 delivery methods (e.g., structured triglycerides or phospholipid conjugates), and iii) include
549 lipidomic and transcriptomic profiling to understand better how DHA and PDN reprogram immune–
550 metabolic networks across disease. Ultimately, well-designed multicenter clinical trials will be
551 essential to determine the translational relevance and clinical significance of DHA-based adjunctive
552 GC-sparing strategies in SLE and LN.

553 ## Conclusion

554 This study provides compelling preclinical evidence that DHA supplementation significantly
555 enhances the efficacy of PDN in sustaining CYC-induced remission in LN. By leveraging a robust,
556 translationally relevant model, we demonstrate that DHA exerts immunomodulatory effects that
557 complement glucocorticoid mechanisms, resulting in prolonged renal and extrarenal protection.
558 These findings highlight the potential of omega-3 fatty acids as safe, cost-effective adjuncts to
559 conventional immunosuppressive regimens, offering a strategy to reduce glucocorticoid burden
560 while improving long-term outcomes. If validated in clinical trials, DHA-based combination therapy
561 could redefine LN management by integrating precision nutrition into standard care, thereby
562 advancing treatment paradigms toward sustained remission with minimized toxicity.

563

564 ## Conflict of Interest

565 The authors declare that the research was conducted in the absence of any commercial or financial
566 relationships that could be construed as a potential conflict of interest.

567

568 ## Author Contributions

569 AA: hypothesis, study design, coordination, animal handling, instillations, urinalysis, necropsy, data
570 curation, data analysis/interpretation, figure preparation, manuscript preparation and submission;
571 OM: animal handling, necropsy, instillations, AAb ELISAs, figure preparation; SJ: animal
572 handling/feeding, injections, urinalysis, diet preparation, sample/data collection, morphometry,
573 figure preparation; JL: animal handling/feeding, diet preparation, data collection; VE: necropsy,

BUN assays, figure preparation; JJ: injections, AAb ELISAs; RL: coordinator, instillations, necropsy, sample histology preparation, slide scanning; JW: necropsy, BALF cell counts; JH: necropsy, oversight, lung/kidney/spleen/brain histopathology, semi-quantitative data analysis, manuscript preparation; JP: hypothesis, study design, oversight, funding acquisition, data analysis/ interpretation, manuscript preparation, and submission.

Funding

This research was funded by NIH ES027353 (AA, JP, JH), DOD HT94252510457 (JP, JH), Lupus Research Alliance Grant 1260473 (AA), and Dr. Robert and Carol Deibel Family Endowment (JP).

Acknowledgments

The authors thank Amy Porter and Kaila Hogg of the Michigan State University Laboratory for Investigative Histopathology for their assistance with histotechnology.

Generative Artificial Intelligence (AI)

Generative AI (Perplexity, Perplexity AI, San Francisco, CA, USA) and Grammarly (Grammarly Inc., San Francisco, CA, USA) were used exclusively for language editing and to improve the clarity, readability, and organization of the manuscript. All scientific content, data interpretation, and conclusions were generated by the authors, who carefully reviewed and edited all AI-assisted text and take full responsibility for the integrity and accuracy of the work

Data Availability Statement

The data supporting the findings of this study are available from the corresponding author upon reasonable request.

600 **Table 1. Formulation of experimental diets.**

	Experimental Diets			
	g/kg Total Diet			
Macronutrients[a]	**CON**	**DHA**	**PDN**	**DHA+PDN**
Carbohydrates				
Corn Starch	397.486	397.486	397.486	397.486
Maltodextrin (Dyetrose)	132	132	132	132
Sucrose	100	100	100	100
Cellulose	50	50	50	50
Proteins				
Casein	200	200	200	200
L-Cysteine	3	3	3	3
Fats				
Corn Oil[b]	10	10	10	10
High-Oleic Safflower Oil[c]	60	35	60	35
DHA-enriched Algal Oil[d]	0	25	0	25
Essential nutrients				
AIN-93G Mineral Mix	35	35	35	35
AIN-93G Vitamin Mix	10	10	10	10
Choline Bitartrate	2.5	2.5	2.5	2.5
Preservatives				
TBHQ Antioxidant	0.014	0.014	0.014	0.014
Drug				
Prednisone	0	0	0.01	0.01

601 Values in table are shown as mass in g/kg diet. Abbreviations: CON: control, DHA: docosahexaenoic acid, PDN:
602 prednisone. [a]Diet composition is based on the manufacturer's description [65]. [b]Corn oil contributes 6 g/kg diet of
603 linoleic acid and 3 g/kg diet of oleic acid. [c]High-oleic safflower oil contributes 47 g/kg diet of oleic acid and 9 g/kg
604 diet of linoleic acid (https://fdc.nal.usda.gov/). [d]Algal oil contributes 10 g/kg diet of DHA and 4 g/kg diet of oleic
605 acid [114]. A 10 g/kg diet of DHA is calorically equivalent to a human equivalent dose of 5 g/d.

606

607 **Table 2. Relation of mouse cyclophosphamide (CYC) injections and dietary**
608 **prednisone (PDN) to human doses.**
609

Drug	Diet concentration (mg/kg)	Mouse dose (mg/kg bw/d)	HED (mg/kg bw/d)[b]	HED (mg/d)[c]
CYC	0	5	0.4	31.2
PDN	10	1.5[a]	0.12	9.36

610 [a]Mouse dose was calculated by multiplying dietary concentration by the FDA conversion factor of 0.15
611 [115].
612 [b]Human equivalent dose (HED) was calculated by multiplying mouse dose by FDA drug interspecies
613 conversion factor of 0.08 [116].
614 [c]Daily human equivalent dose based on average body weight of 78 kg for women ≥ 20 years of age in
615 the U.S. [117].
616

617 **Table 3. Effects of experimental diets on fatty acids in red blood cells (RBCs).**

Chemical Structure	Experimental Group			
	Percent (%) of Total Fatty Acids			
	$cSiO_2$/CYC/CON	$cSiO_2$/CYC/DHA	$cSiO_2$/CYC/PDN	$cSiO_2$/CYC/DHA+PDN
C14:0	0.11 ± 0.02	0.26 ± 0.07**	0.13 ± 0.03	0.30 ± 0.08**
C16:0	25.76 ± 1.6	29.92 ± 0.81****	29.74 ± 1.11	25.76 ± 1.9****
C16:1ω7t	0.05 ± 0.008	0.05 ± 0.005	0.05 ± 0.008	0.05 ± 0.01
C16:1ω7	0.56 ± 0.07	0.67 ± 0.20	0.95 ± 0.22*	1.03 ± 0.20**
C18:0	12.17 ± 1.5	10.83 ± 1.09	10.96 ± 1.53	10.75 ± 0.89
C18:1t	0.12 ± 0.03	0.10 ± 0.02	0.11 ± 0.01	0.08 ± 0.02*
C18:1ω9	23.33 ± 3.56	19.74 ± 1.35	24.63 ± 3.37	17.82 ± 1.26**
C18:2ω6t	0.10 ± 0.02	0.09 ± 0.02	0.14 ± 0.02**	0.09 ± 0.02
C18:2ω6	6.51 ± 1.44	9.14 ± 0.63****	7.49 ± 0.72	8.92 ± 0.89***
C20:0	0.11 ± 0.02	0.10 ± 0.02	0.10 ± 0.01	0.12 ± 0.03
C18:3ω6	0.05 ± 0.02	0.03 ± 0.01*	0.07 ± 0.01**	0.03 ± 0.009*
C20:1ω9	0.46 ± 0.05	0.24 ± 0.02****	0.38 ± 0.08	0.19 ± 0.04****
C18:3ω3	0.01 ± 0	0.01 ± 0.006	0.01 ± 0.007	0.02 ± 0.006
C20:2ω6	0.19 ± 0.04	0.16 ± 0.02	0.16 ± 0.02	0.11 ± 0.02****
C22:0	0.12 ± 0.03	0.14 ± 0.04	0.12 ± 0.02	0.14 ± 0.08
C20:3ω6	1.00 ± 0.10	0.97 ± 0.13	1.14 ± 0.14	0.61 ± 0.13***
C20:4ω6	21.49 ± 2	4.91 ± 0.94****	20.23 ± 2.05	2.40 ± 0.31****
C24:0	0.22 ± 0.06	0.28 ± 0.07	0.23 ± 0.03	0.38 ± 0.06***
C20:5ω3	0.02 ± 0.008	3.66 ± 0.92****	0.03 ± 0.01	5.73 ± 0.85****
C24:1ω9	0.37 ± 0.08	0.35 ± 0.08	0.33 ± 0.04	0.35 ± 0.05
C22:4ω6	2.51 ± 0.57	0.11 ± 0.04**	2.08 ± 0.26	0.04 ± 0.005**
C22:5ω6	2.78 ± 0.70	0.05 ± 0.007**	2.60 ± 0.17	0.03 ± 0.004**
C22:5ω3	0.09 ± 0.03	0.83 ± 0.08****	0.14 ± 0.01	0.91 ± 0.08****
C22:6ω3	1.89 ± 0.23	17.35 ± 1.1****	1.92 ± 0.20	20.17 ± 0.75****
DHA + EPA	1.91 ± 0.24	21.01 ± 1.87****	1.95 ± 0.21	25.9 ± 1.2****
CX:0	38.50 ± 1.65	41.54 ± 0.77**	37.54 ± 1.59	41.42 ± 0.58**
CX:1	24.88 ± 3.51	21.15 ± 1.42	26.46 ± 3.61	19.52 ± 1.4**
CX:≥2ω3	2.01 ± 0.26	21.86 ± 1.93****	2.10 ± 0.21	26.83 ± 1.16****
CX:≥2ω6	34.62 ± 2.51	15.45 ± 1.34****	33.90 ± 2.01	12.24 ± 0.9****

618
619 Fatty acid profiles of RBCs were determined by OmegaQuant Analytics as described in Methods. Data are expressed
620 as mean ± SEM. Symbols: *, **, ***, and **** indicate significant differences at the $p<0.05$, $p<0.01$, $p<0.001$, and
621 $p<0.0001$ levels, respectively, when compared to the $cSiO_2$/CYC/CON group.
622

623 ## Figure Legends

624 **Figure 1.** Experimental design for determining how diets containing docosahexaenoic acid (DHA)
625 and/or prednisone (PDN) impact the duration of cyclophosphamide (CYC)-induced remission in the
626 silica ($cSiO_2$)-accelerated lupus nephritis (SALN) mouse model. Abbreviations: CON, control diet;
627 VEH, vehicle. Letters: a) nephritis onset/initiate vehicle (VEH) or CYC injections; b) CYC
628 discontinued; c) experiment terminated and mice necropsied when ≥50% CYC-treated CON-fed
629 mice exhibited proteinuria (≥300 mg/dl).

630

631 **Figure 2.** Consumption of DHA and DHA+PDN, but not PDN alone, skews cellular phospholipid
632 profiles in erythrocytes from ω-6 PUFAs to ω-3 PUFAs. Data (mean+/-SEM) are expressed as
633 percent of total fatty acids (TFA). *, **, ***, and **** indicate significant differences at the $p<0.05$,
634 $p<0.01$, $p<0.001$, and $p<0.0001$ levels, respectively.

635

636 **Figure 3.** DHA and PDN monotherapies and co-therapy influence the duration of CYC-induced
637 remission of proteinuria and mortality in the SALN model over the 14-week experimental period.
638 (A) Left panel, percent of mice with significant proteinuria (≥300 mg/dl); right panel, average
639 proteinuria. (B) Average percent of mice with proteinuria (≥300 mg/dl) from weeks 21 to 35. (C)
640 Average proteinuria from weeks 21 to 35. (D) Percent survival as determined using clinical scores
641 indicative of a moribund state as described in Methods. Abbreviations: VEH, vehicle; CON, control
642 diet. Symbols: *, **, ***, and **** indicate significant differences at the $p<0.05$, $p<0.01$, $p<0.001$,
643 and $p<0.0001$ levels, respectively.

644

645 **Figure 4.** DHA and PDN monotherapies and co-therapy prolong CYC-induced diminution of $cSiO_2$-
646 accelerated lupus nephritis. (A-F) Light photomicrographs of Periodic Acid Schiff-stained (PAS)

647 glomeruli (g) and adjacent cortical renal tubules (rt). (B) Membranous glomerular nephritis:
648 dramatic glomerular enlargement with marked thickening of PAS^+ membranous tissue (arrow) and
649 rt with luminal proteinaceous fluid (stippled arrow) in the kidney from the $cSiO_2$/VEH/CON mouse
650 compared to (A) a representative section from a 34-week-old NZBWF1 mouse not treated with
651 $cSiO_2$ or drugs obtained from a previous study [61]. These renal lesions are markedly attenuated in
652 the kidney from the (F) $cSiO_2$/CYC/DHA+PDN mouse. Histopathological lesions were scored by
653 pathologist as described in Methods for (G) lupus nephritis, (H) tubular protein, and (I) tubular
654 regeneration. Symbols: #, *, and ** denote statistically significant differences at the $p<0.1$, $p<0.05$,
655 and $p<0.01$ levels, respectively. Solid symbols indicate mice that were taken at the final necropsy at
656 week 35; half-open, half-closed symbols denote moribund mice sacrificed prior to final necropsy.
657
658 **Figure 5.** DHA and PDN co-therapy extends CYC-induced suppression of $cSiO_2$-induced
659 infiltration of inflammatory IBA-1^+ monocyte-derived macrophages in the kidney. (A-F)
660 Representative light photomicrographs of renal cortex immunohistochemically stained for IBA-1^+
661 monocytes infiltrating peri-tubular and glomerular interstitial tissue (arrows). Panel A is a
662 representative section from a 34-week-old NZBWF1 mouse not treated with $cSiO_2$ or drugs obtained
663 from a previous study [61]. Letters: g, glomeruli; rt, renal tubules. (G) IBA-1^+ areas were
664 quantitatively scored as described in Methods. Symbol: * denotes a statistically significant
665 difference at the $p<0.05$ level. Solid symbols indicate mice that were taken at the final necropsy at
666 week 35; half-open, half-closed symbols denote moribund mice sacrificed prior to final necropsy.
667
668 **Figure 6.** DHA and PDN co-therapy prolongs CYC-induced attenuation of $cSiO_2$-accelerated
669 ectopic lymphoid structure (ELS) development in the kidney. Representative light
670 photomicrographs of (A, B) hematoxylin and eosin (H&E)-stained renal cortex tissue and

671 immunohistochemically stained for (C, D) IBA-1$^+$, (E, F) CD3$^+$, or (G, H) CD45R$^+$ cells in renal
672 cortex tissue from a (A, C, E, G) nontreated $cSiO_2$/VEH/CON mouse and a (B, D, F, H) co-treated
673 $cSiO_2$/CYC/DHA+PDN mouse. $cSiO_2$-induced renal influx of IBA-1$^+$ monocytes co-localized with
674 CD3$^+$ and CD45R$^+$ lymphoid cells (T and B cells, respectively) was markedly attenuated in co-
675 treated mouse compared to nontreated mouse. (I) ELS development was semi-quantitatively scored
676 for severity by pathologist as described in Methods. Symbol: * indicates a significant difference at
677 the $p<0.05$ level. Solid symbols indicate mice that were taken at the final necropsy at week 35; half-
678 open, half-closed symbols denote moribund mice sacrificed prior to final necropsy.
679
680 **Figure 7.** Influence of DHA and PDN monotherapies and co-therapy on $cSiO_2$-induced cellularity
681 and AAbs in bronchoalveolar lavage fluid (BALF). (A) Monocyte, neutrophil, lymphocyte, and total
682 cell accumulation are suppressed by DHA and PDN alone or as co-treatment. Symbols: #, *, **,
683 ***, and **** indicate significant differences at the $p<0.1$, $p<0.05$, $p<0.01$, $p<0.001$, and $p<0.0001$
684 levels, respectively. (B) IgG AAbs specific for dsDNA and silica-killed cells (SKC) of CYC-treated
685 mice instilled with $cSiO_2$ are modestly suppressed by DHA and PDN co-treatment.
686
687 **Figure 8.** DHA and PDN monotherapies and co-therapy extend CYC-induced attenuation of $cSiO_2$-
688 accelerated ectopic lymphoid structure (ELS) development in the lung. (A-L) Representative light
689 photomicrographs of H&E-stained pulmonary tissue from the left lung lobe. Panels A and B are a
690 representative section from a 34-week-old NZBWF1 mouse not treated with $cSiO_2$ or drugs obtained
691 from a previous study [61]. Peri-vascular ELS (arrows) is markedly attenuated in lung from (K, L)
692 co-therapy $cSiO_2$/CYC/DHA+PDN mouse compared to (C, D) nontreated $cSiO_2$/VEH/CON and (E,
693 F) $cSiO_2$/CYC/CON mice.
694

695 **Figure 9**. DHA and PDN monotherapies and co-therapy prolong CYC-induced reduction of $cSiO_2$-
696 accelerated ectopic lymphoid structure development in the lung. (A, B) ELS development and
697 alveolar proteinosis were semi-quantitatively scored for severity by pathologist as described in
698 Methods. (C, D) $CD3^+$ and $CD45R^+$ cell densities were quantitatively analyzed by digital
699 morphometry as described in Methods. Symbols: *, **, and *** indicate significant differences at
700 the $p<0.05$, $p<0.01$, and $p<0.001$, levels, respectively. Solid symbols indicate mice that were taken
701 at the final necropsy at week 35; half-open, half-closed symbols denote moribund mice sacrificed
702 prior to final necropsy.
703
704 **Figure 10.** PDN alone or DHA and PDN co-therapy with CYC suppress $cSiO_2$-accelerated
705 splenomegaly. (A-F) Light photomicrographs of H&E-stained splenic tissue. (A) Reference section
706 from a 34-week-old NZBWF1 mouse not treated with $cSiO_2$ or drugs obtained from a previous study
707 [61]. (B) Increased white pulp (wp) and reduced red pulp (rp) in splenic tissue from
708 $cSiO_2$/VEH/CON mouse that is markedly attenuated in (F) spleen from mouse receiving
709 $cSiO_2$/CYC/DHA+PDN treatment. Indicators of splenomegaly included (G) spleen weight, (H)
710 white pulp hyperplasia (semi-quantitative scoring by pathologist as described in Methods), and (I)
711 mid cross-sectional area of total spleen (quantitative analysis as described in Methods). (J) Influence
712 of DHA and PDN monotherapies and co-therapy on $cSiO_2$-induced AAbs in plasma. IgG AAbs
713 specific for dsDNA and silica-killed cells (SKC) from CYC-treated mice instilled with $cSiO_2$ are
714 modestly suppressed by PDN treatment alone and by DHA and PDN co-treatment at 33 and 35
715 weeks. Symbols: #, *, **, and *** indicate significant differences at the $p<0.1$, $p<0.05$, $p<0.01$, and
716 $p<0.001$ levels, respectively. Mice sacrificed prior to final necropsy are indicated by half-open, half-
717 closed symbols, and solid symbols indicate mice that made it to final necropsy at week 35.
718

719 **Figure 11**. DHA and PDN monotherapies and co-therapy prolong CYC suppression of $cSiO_2$-
720 induced microgliosis. Representative photomicrographs of (A) H&E-stained cells and (B-F)
721 immunohistochemically stained for IBA-1^+ microglial cells in the hippocampus of the brain.
722 Microgliosis in the hippocampus from the (B) nontreated $cSiO_2$/VEH/CON mouse is markedly
723 attenuated in (F) co-treated $cSiO_2$/CYC/DHA+PDN mouse. (G) Semi-quantitative severity scoring
724 of microgliosis (IBA-1^+ cells) in the hippocampus as described in Methods. Brains were not taken
725 from moribund mice at necropsy. Symbol: ** indicates a significant difference at the $p<0.01$ level.
726

727 **Figure 12.** Schematic summarizing how docosahexaenoic acid (DHA) supplementation influences
728 prednisone (PDN) efficacy for the sustained maintenance of cyclophosphamide-induced remission
729 in silica-triggered lupus. Inhaled crystalline silica ($cSiO_2$) initiates lung cell death and inflammation,
730 inducing damage-associated molecular patterns (DAMPs), autoantigens (AAgs), type I interferons,
731 and chemokines, which together drive robust infiltration by B cells, T cells, and macrophages,
732 leading to ectopic lymphoid structure formation, AAb production, and immune complex (IC)
733 formation. These immunological events in the lung amplify multiorgan pathology, including
734 glomerulonephritis, IBA-1^+ macrophage accumulation, and lymphoid neogenesis in the kidney,
735 splenic lymphoid hyperplasia, and microgliosis in the brain. Compared to single-agent regimens,
736 combined DHA+PDN therapy exerts superior suppression of multisystem lupus pathology
737 (DHA+PDN > PDN = DHA > control for kidney, lung, and brain; DHA+PDN > PDN > DHA >
738 control for spleen), supporting additive benefits of omega-3 supplementation and long-term
739 maintenance with modest steroid doses to reduce risk of flare and cumulative tissue injury. Figure
740 created using BioRender at https://BioRender.com.
741

References

[1] Tsokos GC. The immunology of systemic lupus erythematosus. Nat Immunol. 2024;25(8):1332-1343.

[2] Woo JMP, Parks CG, Jacobsen S, Costenbader KH, Bernatsky S. The role of environmental exposures and gene-environment interactions in the etiology of systemic lupus erythematous. J Intern Med. 2022;291(6):755-778.

[3] Caielli S, Wan Z, Pascual V. Systemic lupus erythematosus pathogenesis: Interferon and beyond. Annu Rev Immunol. 2023;41:533-560.

[4] Hoi A, Igel T, Mok CC, Arnaud L. Systemic lupus erythematosus. Lancet. 2024;403(10441):2326-2338.

[5] Anders HJ, Saxena R, Zhao MH, Parodis I, Salmon JE, et al. Lupus nephritis. Nat Rev Dis Primers. 2020;6(1):7.

[6] Desai NB, Gashti C, Whittier WL. "A change is gonna come" to treatment of lupus nephritis: A review. Am J Kidney Dis. 2025.

[7] Fanouriakis A, Kostopoulou M, Andersen J, Aringer M, Arnaud L, et al. Eular recommendations for the management of systemic lupus erythematosus: 2023 update. Ann Rheum Dis. 2024;83(1):15-29.

[8] Mok CC, Teng YKO, Saxena R, Tanaka Y. Treatment of lupus nephritis: Consensus, evidence and perspectives. Nat Rev Rheumatol. 2023;19(4):227-238.

[9] Frangou E, Anders HJ, Bajema IM, Teng YKO, Malvar A, et al. Immunosuppression withdrawal in patients with lupus nephritis: When, how, and for whom will it be safe? J Am Soc Nephrol. 2024;35(7):955-958.

[10] Newman TV, Guo J, Hernandez I. Emerging treatments for lupus nephritis: Health equity considerations in clinical research and coverage. J Manag Care Spec Pharm. 2021;27(10):1500-1502.

[11] Nicastro HL, Vorkoper S, Sterling R, Korn AR, Brown AGM, et al. Opportunities to advance implementation science and nutrition research: A commentary on the strategic plan for nih nutrition research. Transl Behav Med. 2023;13(1):1-6.

[12] Shanmugam VK, Ufret-Vincenty C, Li X, Clayton JA. The inaugural nih-wide strategic plan for autoimmune disease research (fy2026–2030). Arthr Rheumatol.4.

[13] Robinson GA, McDonnell T, Wincup C, Martin-Gutierrez L, Wilton J, et al. Diet and lupus: What do the patients think? Lupus. 2019;28(6):755-763.

[14] Ramessar N, Borad A, Schlesinger N. The effect of omega-3 fatty acid supplementation in systemic lupus erythematosus patients: A systematic review. Lupus. 2022;31(3):287-296.

[15] Salek M, Hosseini Hooshiar S, Salek M, Poorebrahimi M, Jafarnejad S. Omega-3 fatty acids: Current insights into mechanisms of action in systemic lupus erythematosus. Lupus. 2023;32(1):7-22.

[16] Salmon J, Wallace DJ, Rus V, Cox A, Dykas C, et al. Correction of omega-3 fatty acid deficiency and improvement in disease activity in patients with systemic lupus erythematosus treated with krill oil concentrate: A multicentre, randomised, double-blind, placebo-controlled trial. Lupus Sci Med. 2024;11(2).

[17] Calder PC. Omega-3 fatty acids and inflammatory processes: From molecules to man. Biochem Soc Trans. 2017;45(5):1105-1115.

[18] Bodur M, Yilmaz B, Ağagündüz D, Ozogul Y. Immunomodulatory effects of omega-3 fatty acids: Mechanistic insights and health implications. Mol Nutr Food Res. 2025;69(10):e202400752.
[19] Djuricic I, Calder PC. Pros and cons of long-chain omega-3 polyunsaturated fatty acids in cardiovascular health. Annu Rev Pharmacol Toxicol. 2023;63:383-406.
[20] Laguzzi F, Åkesson A, Marklund M, Qian F, Gigante B, et al. Role of polyunsaturated fat in modifying cardiovascular risk associated with family history of cardiovascular disease: Pooled de novo results from 15 observational studies. Circulation. 2024;149(4):305-316.
[21] O'Keefe JH, Tintle NL, Harris WS, O'Keefe EL, Sala-Vila A, et al. Omega-3 blood levels and stroke risk: A pooled and harmonized analysis of 183 291 participants from 29 prospective studies. Stroke. 2024;55(1):50-58.
[22] Akbar U, Yang M, Kurian D, Mohan C. Omega-3 fatty acids in rheumatic diseases: A critical review. J Clin Rheumatol. 2017;23(6):330-339.
[23] Sigaux J, Mathieu S, Nguyen Y, Sanchez P, Letarouilly JG, et al. Impact of type and dose of oral polyunsaturated fatty acid supplementation on disease activity in inflammatory rheumatic diseases: A systematic literature review and meta-analysis. Arthritis Res Ther. 2022;24(1):100.
[24] EFSA Panel on Dietetic Products N, Allergies. Scientific opinion on the tolerable upper intake level of eicosapentaenoic acid (epa), docosahexaenoic acid (dha) and docosapentaenoic acid (dpa). EFSA Journal. 2012;10(7):2815.
[25] Kennedy ET, Luo H, Ausman LM. Cost implications of alternative sources of (n-3) fatty acid consumption in the united states1234. The Journal of Nutrition. 2012;142(3):605S-609S.
[26] Wierenga KA, Strakovsky RS, Benninghoff AD, Rajasinghe LD, Lock AL, et al. Requisite omega-3 hufa biomarker thresholds for preventing murine lupus flaring. Front Immunol. 2020;11:1796.
[27] Heine LK, Nault R, Jackson J, Anderson AN, Harkema JR, et al. Omega-3 fatty acid synergy with glucocorticoid in mouse lupus macrophage model: Targeting pathogenic pathways to reduce steroid dependence. Front Immunol. 2025;16:1646133.
[28] Alexander NJ, Smythe NL, Jokinen MP. The type of dietary fat affects the severity of autoimmune disease in nzb/nzw mice. Am J Pathol. 1987;127(1):106-21.
[29] Bhattacharya A, Lawrence RA, Krishnan A, Zaman K, Sun D, et al. Effect of dietary n-3 and n-6 oils with and without food restriction on activity of antioxidant enzymes and lipid peroxidation in livers of cyclophosphamide treated autoimmune-prone nzb/w female mice. J Am Coll Nutr. 2003;22(5):388-99.
[30] Blok WL, Katan MB, van der Meer JW. Modulation of inflammation and cytokine production by dietary (n-3) fatty acids. J Nutr. 1996;126(6):1515-33.
[31] Chandrasekar B, Troyer DA, Venkatraman JT, Fernandes G. Dietary omega-3 lipids delay the onset and progression of autoimmune lupus nephritis by inhibiting transforming growth factor beta mrna and protein expression. J Autoimmun. 1995;8(3):381-93.
[32] Clark WF, Parbtani A. Omega-3 fatty acid supplementation in clinical and experimental lupus nephritis. Am J Kidney Dis. 1994;23(5):644-7.
[33] Fernandes G, Bysani C, Venkatraman JT, Tomar V, Zhao W. Increased tgf-beta and decreased oncogene expression by omega-3 fatty acids in the spleen delays onset of autoimmune disease in b/w mice. J Immunol. 1994;152(12):5979-87.
[34] Fernandes G, Chandrasekar B, Luan X, Troyer DA. Modulation of antioxidant enzymes and programmed cell death by n-3 fatty acids. Lipids. 1996;31 Suppl(3 SUPPL.):S91-6.

[35] Godfrey DG, Stimson WH, Watson J, Belch JF, Sturrock RD. Effects of dietary supplementation on autoimmunity in the mrl/lpr mouse: A preliminary investigation. Ann Rheum Dis. 1986;45(12):1019-24.
[36] Halade GV, Rahman MM, Bhattacharya A, Barnes JL, Chandrasekar B, et al. Docosahexaenoic acid-enriched fish oil attenuates kidney disease and prolongs median and maximal life span of autoimmune lupus-prone mice. J Immunol. 2010;184(9):5280-6.
[37] Halade GV, Williams PJ, Veigas JM, Barnes JL, Fernandes G. Concentrated fish oil (lovaza(r)) extends lifespan and attenuates kidney disease in lupus-prone short-lived (nzb x nzw)f1 mice. Exp Biol Med 2013;238(6):610-622.
[38] Jolly CA, Fernandes G. Diet modulates th-1 and th-2 cytokine production in the peripheral blood of lupus-prone mice. J Clin Immunol. 1999;19(3):172-8.
[39] Jolly CA, Muthukumar A, Reddy Avula CP, Fernandes G. Maintenance of nf-kappab activation in t-lymphocytes and a naive t-cell population in autoimmune-prone (nzb/nzw)f(1) mice by feeding a food-restricted diet enriched with n-3 fatty acids. Cell Immunol. 2001;213(2):122-33.
[40] Kelley VE, Ferretti A, Izui S, Strom TB. A fish oil diet rich in eicosapentaenoic acid reduces cyclooxygenase metabolites, and suppresses lupus in mrl-lpr mice. J Immunol. 1985;134(3):1914-9.
[41] Kobayashi A, Ito A, Shirakawa I, Tamura A, Tomono S, et al. Dietary supplementation with eicosapentaenoic acid inhibits plasma cell differentiation and attenuates lupus autoimmunity. Front Immunol. 2021;12:650856.
[42] Lim BO, Jolly CA, Zaman K, Fernandes G. Dietary (n-6) and (n-3) fatty acids and energy restriction modulate mesenteric lymph node lymphocyte function in autoimmune-prone (nzb x nzw)f1 mice. J Nutr. 2000;130(7):1657-64.
[43] Cheng Y, Liu L, Ye Y, He Y, Hu W, et al. Roles of macrophages in lupus nephritis. Front Pharmacol. 2024;15:1477708.
[44] Pestka JJ, Vines LL, Bates MA, He K, Langohr I. Comparative effects of n-3, n-6 and n-9 unsaturated fatty acid-rich diet consumption on lupus nephritis, autoantibody production and cd4+ t cell-related gene responses in the autoimmune nzbwf1 mouse. PLoS One. 2014;9(6):e100255.
[45] Prickett JD, Robinson DR, Steinberg AD. A diet enriched with eicosapentaenoic acid suppresses autoimmune nephritis in female (nzb x nzw) f1 mice. Trans Assoc Am Physicians. 1982;95:145-54.
[46] Reddy Avula CP, Lawrence RA, Zaman K, Fernandes G. Inhibition of intracellular peroxides and apoptosis of lymphocytes in lupus-prone b/w mice by dietary n-6 and n-3 lipids with calorie restriction. J Clin Immunol. 2002;22(4):206-19.
[47] Robinson DR, Hirai A, Steinberg AD, Colvin RB. Alleviation of murine autoimmune disease by dietary marine lipids. Adv Prostaglandin Thromboxane Leukot Res. 1987;17B:850-3.
[48] Robinson DR, Prickett JD, Polisson R, Steinberg AD, Levine L. The protective effect of dietary fish oil on murine lupus. Prostaglandins. 1985;30(1):51-75.
[49] Robinson DR, Xu LL, Tateno S, Guo M, Colvin RB. Suppression of autoimmune disease by dietary n-3 fatty acids. J Lipid Res. 1993;34(8):1435-44.
[50] Spurney RF, Ruiz P, Albrightson CR, Pisetsky DS, Coffman TM. Fish oil feeding modulates leukotriene production in murine lupus nephritis. Prostaglandins. 1994;48(5):331-48.

879 [51] Venkatraman JT, Chu WC. Effects of dietary omega-3 and omega-6 lipids and vitamin e on
880 serum cytokines, lipid mediators and anti-DNA antibodies in a mouse model for rheumatoid
881 arthritis. J Am Coll Nutr. 1999;18(6):602-13.
882 [52] Watson J, Godfrey D, Stimson WH, Belch JJ, Sturrock RD. The therapeutic effects of dietary
883 fatty acid supplementation in the autoimmune disease of the mrl-mp-lpr/lpr mouse. Int J
884 Immunopharmacol. 1988;10(4):467-71.
885 [53] Westberg G, Tarkowski A, Svalander C. Effect of eicosapentaenoic acid rich menhaden oil
886 and maxepa on the autoimmune disease of mrl/l mice. Int Arch Allergy Appl Immunol.
887 1989;88(4):454-61.
888 [54] Bates MA, Brandenberger C, Langohr I, Kumagai K, Harkema JR, et al. Silica triggers
889 inflammation and ectopic lymphoid neogenesis in the lungs in parallel with accelerated onset
890 of systemic autoimmunity and glomerulonephritis in the lupus-prone nzbwf1 mouse. PLoS
891 One. 2015;10(5):e0125481.
892 [55] Bates MA, Benninghoff AD, Gilley KN, Holian A, Harkema JR, et al. Mapping of dynamic
893 transcriptome changes associated with silica-triggered autoimmune pathogenesis in the
894 lupus-prone nzbwf1 mouse. Front Immunol. 2019;10:632.
895 [56] Bates MA, Brandenberger C, Langohr, II, Kumagai K, Lock AL, et al. Silica-triggered
896 autoimmunity in lupus-prone mice blocked by docosahexaenoic acid consumption. PLoS
897 One. 2016;11(8):e0160622.
898 [57] Bates MA, Akabari P, Gilley KN, Wagner JG, Li N, et al. Dietary docosahexaenoic acid
899 prevents silica-induced development of pulmonary ectopic germinal centers and
900 glomerulonephritis in the lupus-prone nzbwf1 mouse. Front Immunol. 2018;9:2002.
901 [58] Benninghoff AD, Bates MA, Chauhan PS, Wierenga KA, Gilley KN, et al. Docosahexaenoic
902 acid consumption impedes early interferon- and chemokine-related gene expression while
903 suppressing silica-triggered flaring of murine lupus. Front Immunol. 2019;10:2851.
904 [59] Gilley KN, Wierenga KA, Chauhuan PS, Wagner JG, Lewandowski RP, et al. Influence of
905 total western diet on docosahexaenoic acid suppression of silica-triggered lupus flaring in
906 nzbwf1 mice. PLoS One. 2020;15(5):e0233183.
907 [60] Rajasinghe LD, Li QZ, Zhu C, Yan M, Chauhan PS, et al. Omega-3 fatty acid intake
908 suppresses induction of diverse autoantibody repertoire by crystalline silica in lupus-prone
909 mice. Autoimmunity. 2020;53(7):415-433.
910 [61] Pestka JJ, Akbari P, Wierenga KA, Bates MA, Gilley KN, et al. Omega-3 polyunsaturated
911 fatty acid intervention against established autoimmunity in a murine model of toxicant-
912 triggered lupus. Front Immunol. 2021;12:653464.
913 [62] Rajasinghe LD, Bates MA, Benninghoff AD, Wierenga KA, Harkema JR, et al. Silica
914 induction of diverse inflammatory proteome in lungs of lupus-prone mice quelled by dietary
915 docosahexaenoic acid supplementation. Front Immunol. 2021;12:781446.
916 [63] Chauhan PS, Benninghoff AD, Favor OK, Wagner JG, Lewandowski RP, et al. Dietary
917 docosahexaenoic acid supplementation inhibits acute pulmonary transcriptional and
918 autoantibody responses to a single crystalline silica exposure in lupus-prone mice. Front
919 Immunol. 2024;15:1275265.
920 [64] Heine LK, Benninghoff AD, Ross EA, Rajasinghe LD, Wagner JG, et al. Comparative
921 effects of human-equivalent low, moderate, and high dose oral prednisone intake on
922 autoimmunity and glucocorticoid-related toxicity in a murine model of environmental-
923 triggered lupus. Front Immunol. 2022;13:972108.

[65] Reeves PG, Nielsen FH, Fahey GC, Jr. Ain-93 purified diets for laboratory rodents: Final report of the american institute of nutrition ad hoc writing committee on the reformulation of the ain-76a rodent diet. J Nutr. 1993;123(11):1939-51.
[66] Buttgereit F, Da Silva JAP, Boers M, Burmester GR, Cutolo M, et al. Standardised nomenclature for glucocorticoid dosages and glucocorticoid treatment regimens: Current questions and tentative answers in rheumatology. Annals of the Rheumatic Diseases. 2002;61(8):718-722.
[67] OSHA. Osha's final rule to protect workers from exposure to respirable crystalline silica2016 [cited 16286 - 16890 p.]. https://www.federalregister.gov/documents/2016/03/25/2016-04800/occupational-exposure-to-respirable-crystalline-silica
[68] Bankhead P, Loughrey MB, Fernández JA, Dombrowski Y, McArt DG, et al. Qupath: Open source software for digital pathology image analysis. Sci Rep. 2017;7(1):16878.
[69] Meyerholz DK, Beck AP. Fundamental concepts for semiquantitative tissue scoring in translational research. ILAR J. 2018;59(1):13-17.
[70] McDonald OF, Wagner JG, Lewandowski RP, Heine LK, Estrada V, et al. Impact of soluble epoxide hydrolase inhibition on silica-induced pulmonary fibrosis, ectopic lymphoid neogenesis, and autoantibody production in lupus-prone mice. Inhal Toxicol. 2024;36(7-8):442-460.
[71] Harris WS. Recent studies confirm the utility of the omega-3 index. Curr Opin Clin Nutr Metab Care. 2025;28(2):91-95.
[72] Ohsawa K, Imai Y, Sasaki Y, Kohsaka S. Microglia/macrophage-specific protein iba1 binds to fimbrin and enhances its actin-bundling activity. J Neurochem. 2004;88(4):844-56.
[73] Wang M, Rajkumar S, Lai Y, Liu X, He J, et al. Tertiary lymphoid structures as local perpetuators of organ-specific immune injury: Implication for lupus nephritis. Front Immunol. 2023;14:1204777.
[74] Masum MA, Ichii O, Elewa YHA, Otani Y, Namba T, et al. Vasculature-associated lymphoid tissue: A unique tertiary lymphoid tissue correlates with renal lesions in lupus nephritis mouse model. Front Immunol. 2020;11:595672.
[75] Dorraji SE, Kanapathippillai P, Hovd AK, Stenersrød MR, Horvei KD, et al. Kidney tertiary lymphoid structures in lupus nephritis develop into large interconnected networks and resemble lymph nodes in gene signature. Am J Pathol. 2020;190(11):2203-2225.
[76] Harbeck RJ, Launder T, Staszak C. Mononuclear cell pulmonary vasculitis in nzb/w mice. Ii. Immunohistochemical characterization of the infiltrating cells. Am J Pathol. 1986;123(2):204-11.
[77] Staszak C, Harbeck RJ. Mononuclear-cell pulmonary vasculitis in nzb/w mice. I. Histopathologic evaluation of spontaneously occurring pulmonary infiltrates. Am J Pathol. 1985;120(1):99-105.
[78] Wierenga KA, Harkema JR, Pestka JJ. Lupus, silica, and dietary omega-3 fatty acid interventions. Toxicol Pathol. 2019;47(8):1004-1011.
[79] Ye YL, Chiang BL. Reconstitution of severe combined immunodeficient mice with spleen cells from autoimmune nzbxnzw f1 mice. Clin Exp Rheumatol. 1998;16(1):33-7.
[80] Nikolopoulos D, Manolakou T, Polissidis A, Filia A, Bertsias G, et al. Microglia activation in the presence of intact blood-brain barrier and disruption of hippocampal neurogenesis via il-6 and il-18 mediate early diffuse neuropsychiatric lupus. Ann Rheum Dis. 2023;82(5):646-657.

[81] Nomura A, Noto D, Murayama G, Chiba A, Miyake S. Unique primed status of microglia under the systemic autoimmune condition of lupus-prone mice. Arthritis Res Ther. 2019;21(1):303.
[82] Rodríguez-Gómez JA, Kavanagh E, Engskog-Vlachos P, Engskog MKR, Herrera AJ, et al. Microglia: Agents of the cns pro-inflammatory response. Cells. 2020;9(7):1717.
[83] Charoenwoodhipong P, Harlow SD, Marder W, Hassett AL, McCune WJ, et al. Dietary omega polyunsaturated fatty acid intake and patient-reported outcomes in systemic lupus erythematosus: The michigan lupus epidemiology and surveillance program. Arthritis Care Res (Hoboken). 2020;72(7):874-881.
[84] Vordenbaumen S, Sokolowski A, Kutzner L, Rund KM, Dusing C, et al. Erythrocyte membrane polyunsaturated fatty acid profiles are associated with systemic inflammation and fish consumption in systemic lupus erythematosus: A cross-sectional study. Lupus. 2020;29(6):554-559.
[85] Gilley KF, JI; Zick, SM; Li, K; , Wang LM, W; , Mccune WJ, R; Herndon-Fenton,S; Hassett,A; Barbour, K; Pestka, J.J.;Somers, EC;. Serum fatty acid profiles in systemic lupus erythematosus and patient reported outcomes: The michigan lupus epidemiology & surveillance (miles) program. Frontiers in Immunology. 2024;15.
[86] Arriens C, Hynan LS, Lerman RH, Karp DR, Mohan C. Placebo-controlled randomized clinical trial of fish oil's impact on fatigue, quality of life, and disease activity in systemic lupus erythematosus. Nutr J. 2015;14:82.
[87] Duffy EM, Meenagh GK, McMillan SA, Strain JJ, Hannigan BM, et al. The clinical effect of dietary supplementation with omega-3 fish oils and/or copper in systemic lupus erythematosus. J Rheumatol. 2004;31(8):1551-6.
[88] Lozovoy MA, Simão AN, Morimoto HK, Scavuzzi BM, Iriyoda TV, et al. Fish oil n-3 fatty acids increase adiponectin and decrease leptin levels in patients with systemic lupus erythematosus. Mar Drugs. 2015;13(2):1071-83.
[89] Walton AJ, Snaith ML, Locniskar M, Cumberland AG, Morrow WJ, et al. Dietary fish oil and the severity of symptoms in patients with systemic lupus erythematosus. Ann Rheum Dis. 1991;50(7):463-6.
[90] Wright SA, O'Prey FM, McHenry MT, Leahey WJ, Devine AB, et al. A randomised interventional trial of omega-3-polyunsaturated fatty acids on endothelial function and disease activity in systemic lupus erythematosus. Ann Rheum Dis. 2008;67(6):841-8.
[91] Westberg G, Tarkowski A. Effect of maxepa in patients with sle. A double-blind, crossover study. Scand J Rheumatol. 1990;19(2):137-43.
[92] Bello KJ, Fang H, Fazeli P, Bolad W, Corretti M, et al. Omega-3 in sle: A double-blind, placebo-controlled randomized clinical trial of endothelial dysfunction and disease activity in systemic lupus erythematosus. Rheumatol Int. 2013;33(11):2789-96.
[93] Clark WF, Parbtani A, Huff MW, Reid B, Holub BJ, et al. Omega-3 fatty acid dietary supplementation in systemic lupus erythematosus. Kidney Int. 1989;36(4):653-60.
[94] Favor OK, Pestka JJ, Bates MA, Lee KSS. Centrality of myeloid-lineage phagocytes in particle-triggered inflammation and autoimmunity. Front Toxicol. 2021;3:777768.
[95] Heine LK, Scarlett T, Wagner JG, Lewandowski RP, Benninghoff AD, et al. Crystalline silica-induced pulmonary inflammation and autoimmunity in mature adult nzbw/f1 mice: Age-related sensitivity and impact of omega-3 fatty acid intervention. Inhal Toxicol. 2024;36(2):106-123.
[96] Calder PC. Omega-3 polyunsaturated fatty acids and inflammatory processes: Nutrition or pharmacology? Br J Clin Pharmacol. 2013;75(3):645-62.

1016 [97] Djuricic I, Calder PC. Beneficial outcomes of omega-6 and omega-3 polyunsaturated fatty
1017 acids on human health: An update for 2021. Nutrients. 2021;13(7):2421.
1018 [98] Pennington ER, Virk R, Bridges MD, Bathon BE, Beatty N, et al. Docosahexaenoic acid
1019 controls pulmonary macrophage lipid raft size and inflammation. J Nutr. 2024;154(6):1945-
1020 1958.
1021 [99] Wierenga KA, Riemers FM, Westendorp B, Harkema JR, Pestka JJ. Single cell analysis of
1022 docosahexaenoic acid suppression of sequential lps-induced proinflammatory and
1023 interferon-regulated gene expression in the macrophage. Front Immunol. 2022;13:993614.
1024 [100] Chang HY, Lee HN, Kim W, Surh YJ. Docosahexaenoic acid induces m2 macrophage
1025 polarization through peroxisome proliferator-activated receptor gamma activation. Life Sci.
1026 2015;120:39-47.
1027 [101] Ralston JC, Matravadia S, Gaudio N, Holloway GP, Mutch DM. Polyunsaturated fatty acid
1028 regulation of adipocyte fads1 and fads2 expression and function. Obesity. 2015;23(4):725-
1029 728.
1030 [102] Furst R, Schroeder T, Eilken HM, Bubik MF, Kiemer AK, et al. Mapk phosphatase-1
1031 represents a novel anti-inflammatory target of glucocorticoids in the human endothelium.
1032 FASEB J. 2007;21(1):74-80.
1033 [103] Cain DW, Cidlowski JA. Immune regulation by glucocorticoids. Nat Rev Immunol.
1034 2017;17(4):233-247.
1035 [104] Vandewalle J, Luypaert A, De Bosscher K, Libert C. Therapeutic mechanisms of
1036 glucocorticoids. Trends Endocrinol Metab. 2018;29(1):42-54.
1037 [105] Cain DW, Cidlowski JA. Immune regulation by glucocorticoids. Nature Publishing Group;
1038 2017. p. 233-247.
1039 [106] Atkovska K, Klingler J, Oberwinkler J, Keller S, Hub JS. Rationalizing steroid interactions
1040 with lipid membranes: Conformations, partitioning, and kinetics. ACS Cent Sci.
1041 2018;4(9):1155-1165.
1042 [107] Yamagata S, Tomita K, Sano H, Itoh Y, Fukai Y, et al. Non-genomic inhibitory effect of
1043 glucocorticoids on activated peripheral blood basophils through suppression of lipid raft
1044 formation. Clin Exp Immunol. 2012;170(1):86-93.
1045 [108] Van Laethem F, Liang X, Andris F, Urbain J, Vandenbranden M, et al. Glucocorticoids alter
1046 the lipid and protein composition of membrane rafts of a murine t cell hybridoma. J
1047 Immunol. 2003;170(6):2932-9.
1048 [109] Mok TC, Mok CC. Glucocorticoid in systemic lupus erythematosus: The art beyond science.
1049 Expert Rev Clin Immunol. 2025;21(5):543-553.
1050 [110] Birt JA, Wu J, Griffing K, Bello N, Princic N, et al. Corticosteroid dosing and opioid use are
1051 high in patients with sle and remain elevated after belimumab initiation: A retrospective
1052 claims database analysis. Lupus Sci Med. 2020;7(1).
1053 [111] Li Y, Lee PY, Reeves WH. Monocyte and macrophage abnormalities in systemic lupus
1054 erythematosus. Arch Immunol Ther Exp (Warsz). 2010;58(5):355-64.
1055 [112] Udalova IA, Mantovani A, Feldmann M. Macrophage heterogeneity in the context of
1056 rheumatoid arthritis. Nat Rev Rheumatol. 2016;12(8):472-85.
1057 [113] Northcott M, Jones S, Koelmeyer R, Bonin J, Vincent F, et al. Type 1 interferon status in
1058 systemic lupus erythematosus: A longitudinal analysis. Lupus Sci Med. 2022;9(1):e000625.
1059 [114] USFDA. Gras notice (grn) no. 553: Algal oil (40% docosahexaenoic acid) derived from
1060 schizochytrium sp. Silver Spring, MD: U.S. Food and Drug Administration, Center for Food
1061 Safety and Applied Nutrition; 2015.

1062 [115] Lehman AJ. Approximate relation of parts per million in the diet to mg/kg bw/day.
1063 Association of Food and Drug Officials Quarterly Bulletin. 1954 18.
1064 [116] FDA. Estimating the safe starting dose in clinical trials for therapeutics in adult healthy
1065 volunteers.: U.S. Department of Health and Human Services 2005. Available from:
1066 https://www.fda.gov/regulatory-information/search-fda-guidance-documents/estimating-
1067 maximum-safe-starting-dose-initial-clinical-trials-therapeutics-adult-healthy-volunteers
1068 [117] Fryar C, Carroll M, Gu Q, Afful J, Ogden C. Anthropometric reference data for children and
1069 adults: United states, 2015–2018. National Center for Health Statistics Vital Health Stat
1070 2021;3(46).

1071

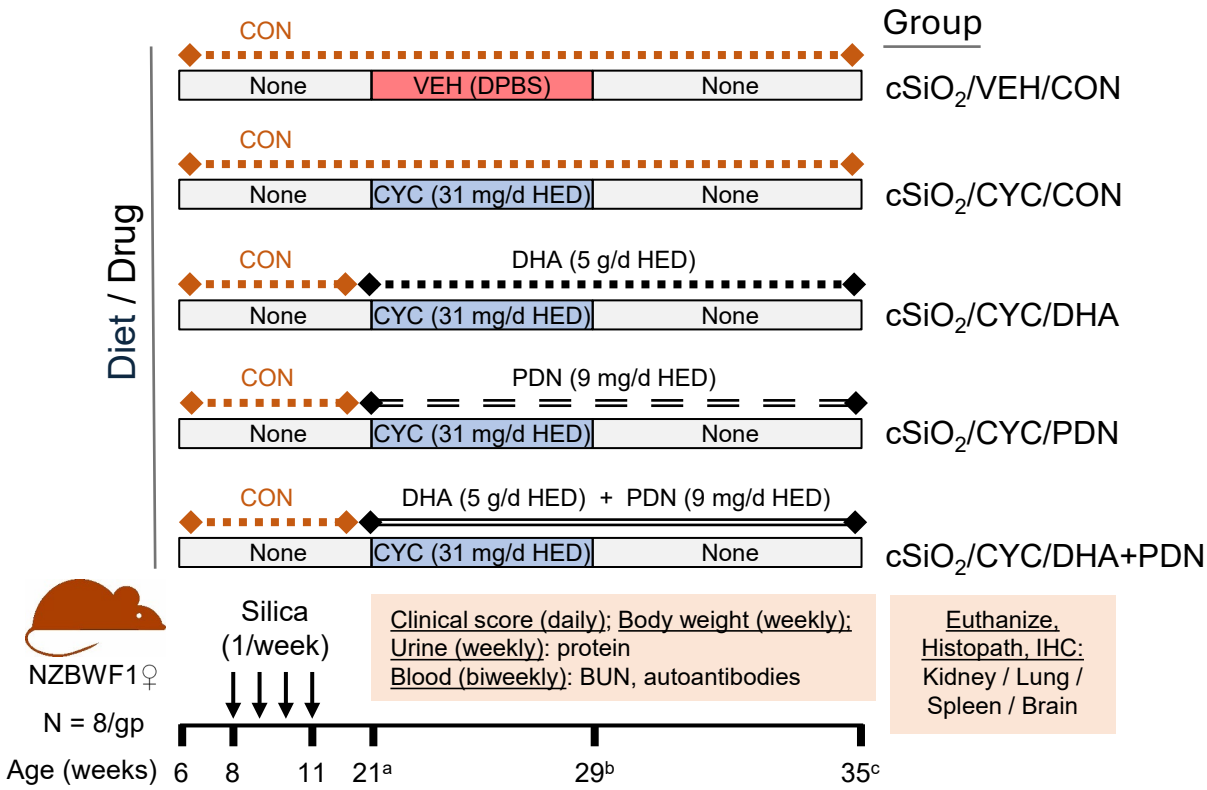
Group
Diet / Drug
CON
None
VEH (DPBS)
None
cSiO2/VEH/CON
CON
None
CYC (31 mg/d HED)
None
cSiO2/CYC/CON
CON
DHA (5 g/d HED)
None
CYC (31 mg/d HED)
None
cSiO2/CYC/DHA
CON
PDN (9 mg/d HED)
None
CYC (31 mg/d HED)
None
cSiO2/CYC/PDN
CON
DHA (5 g/d HED) + PDN (9 mg/d HED)
None
CYC (31 mg/d HED)
None
cSiO2/CYC/DHA+PDN
NZBWF1♀
N = 8/gp
Silica
(1/week)
Clinical score (daily); Body weight (weekly);
Urine (weekly): protein
Blood (biweekly): BUN, autoantibodies
Euthanize,
Histopath, IHC:
Kidney / Lung /
Spleen / Brain
Age (weeks)
6
8
11
21a
29b
35c

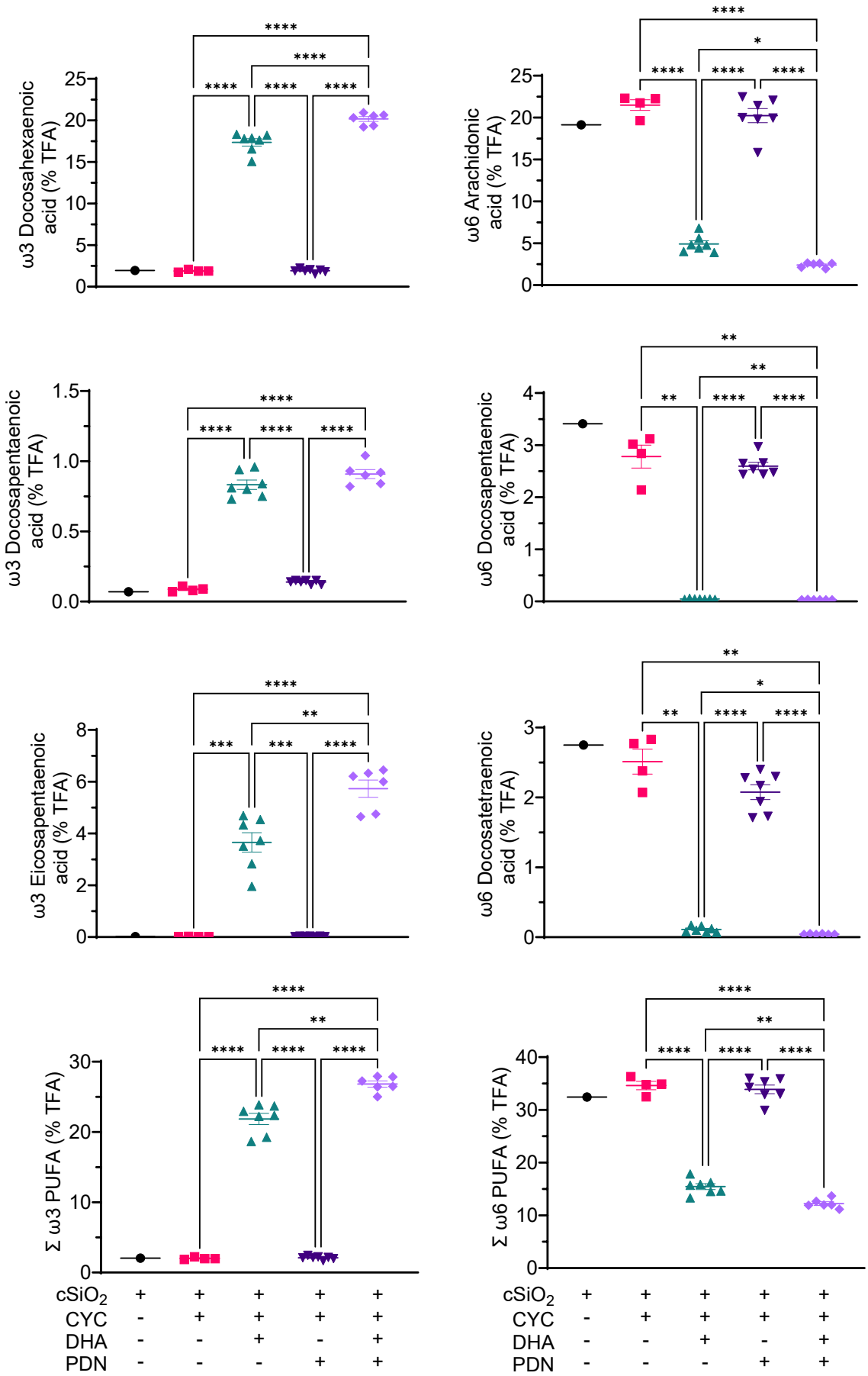
ω3 Docosahexaenoic acid (% TFA)
ω6 Arachidonic acid (% TFA)
ω3 Docosapentaenoic acid (% TFA)
ω6 Docosapentaenoic acid (% TFA)
ω3 Eicosapentaenoic acid (% TFA)
ω6 Docosatetraenoic acid (% TFA)
Σ ω3 PUFA (% TFA)
Σ ω6 PUFA (% TFA)
cSiO2 + + + + +
CYC - + + + +
DHA - - + - +
PDN - - - + +

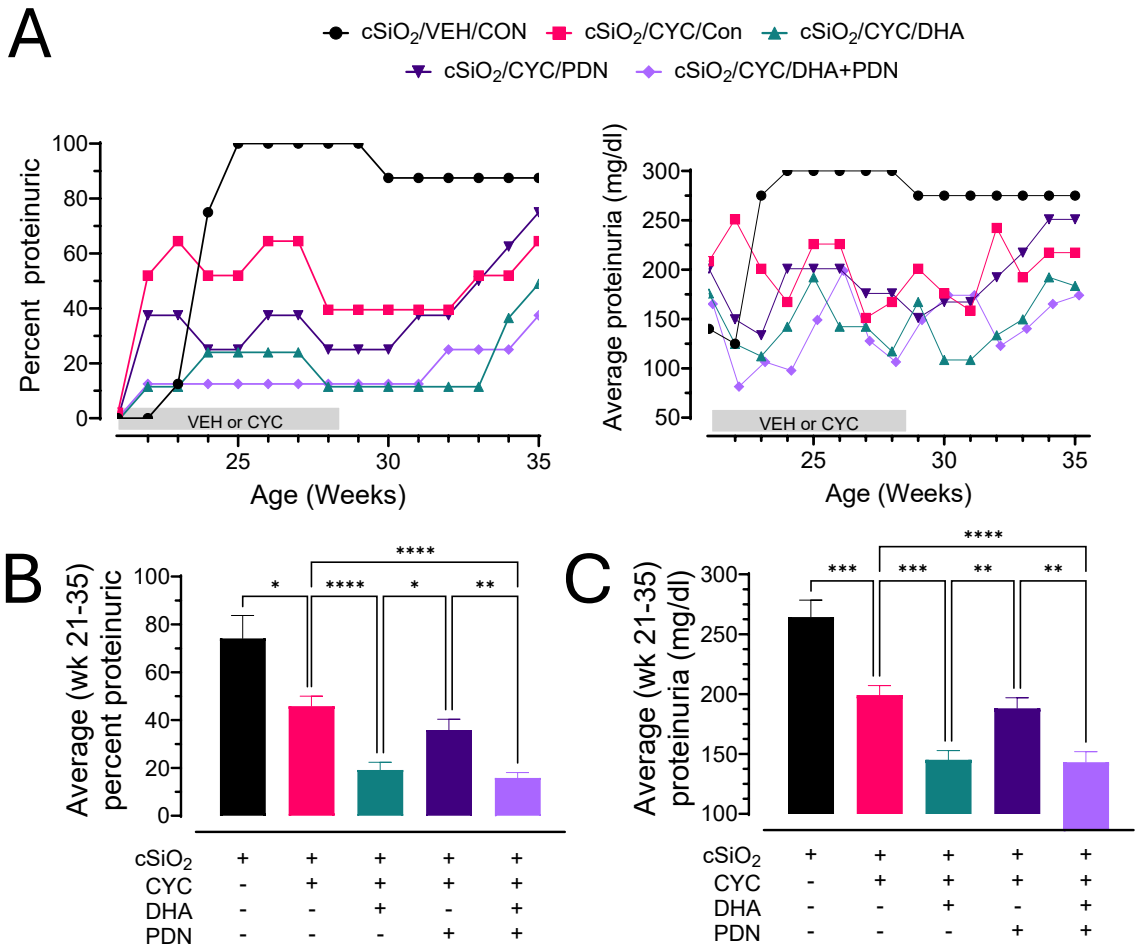
A
cSiO2/VEH/CON
cSiO2/CYC/Con
cSiO2/CYC/DHA
cSiO2/CYC/PDN
cSiO2/CYC/DHA+PDN
Percent proteinuric
Average proteinuria (mg/dl)
VEH or CYC
Age (Weeks)
B
Average (wk 21-35) percent proteinuric
C
Average (wk 21-35) proteinuria (mg/dl)
cSiO2
CYC
DHA
PDN

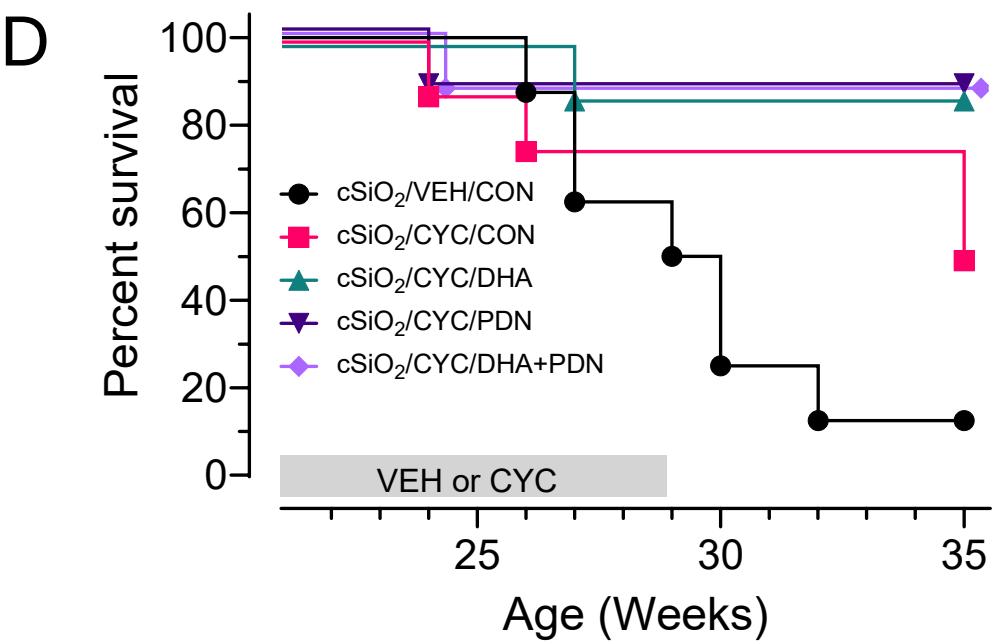
D
Percent survival
cSiO2/VEH/CON
cSiO2/CYC/CON
cSiO2/CYC/DHA
cSiO2/CYC/PDN
cSiO2/CYC/DHA+PDN
VEH or CYC
Age (Weeks)

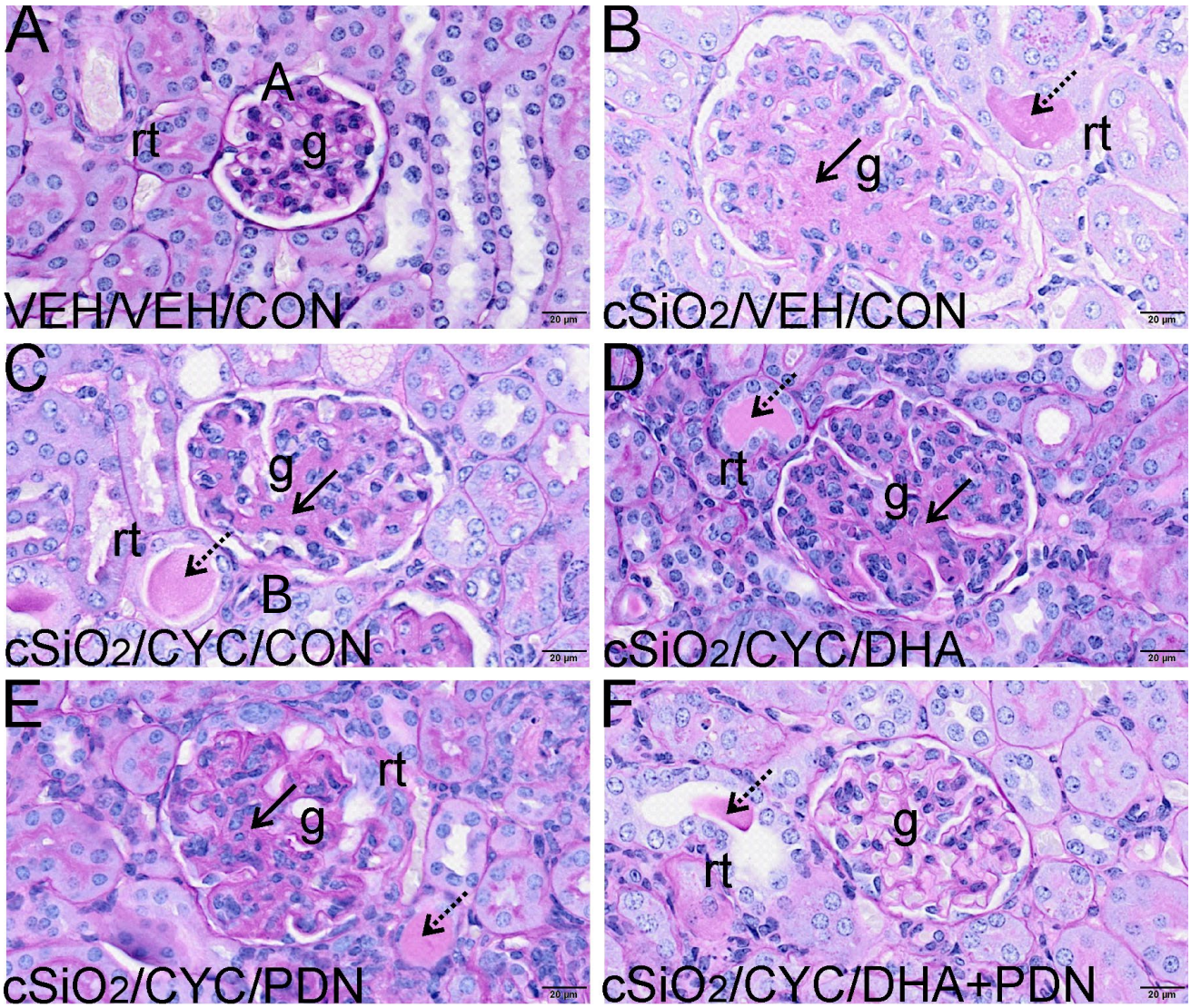
A
A
rt
g
VEH/VEH/CON
20 µm
B
rt
g
cSiO2/VEH/CON
20 µm
C
g
rt
B
cSiO2/CYC/CON
20 µm
D
rt
g
cSiO2/CYC/DHA
20 µm
E
rt
g
cSiO2/CYC/PDN
20 µm
F
g
rt
cSiO2/CYC/DHA+PDN
20 µm

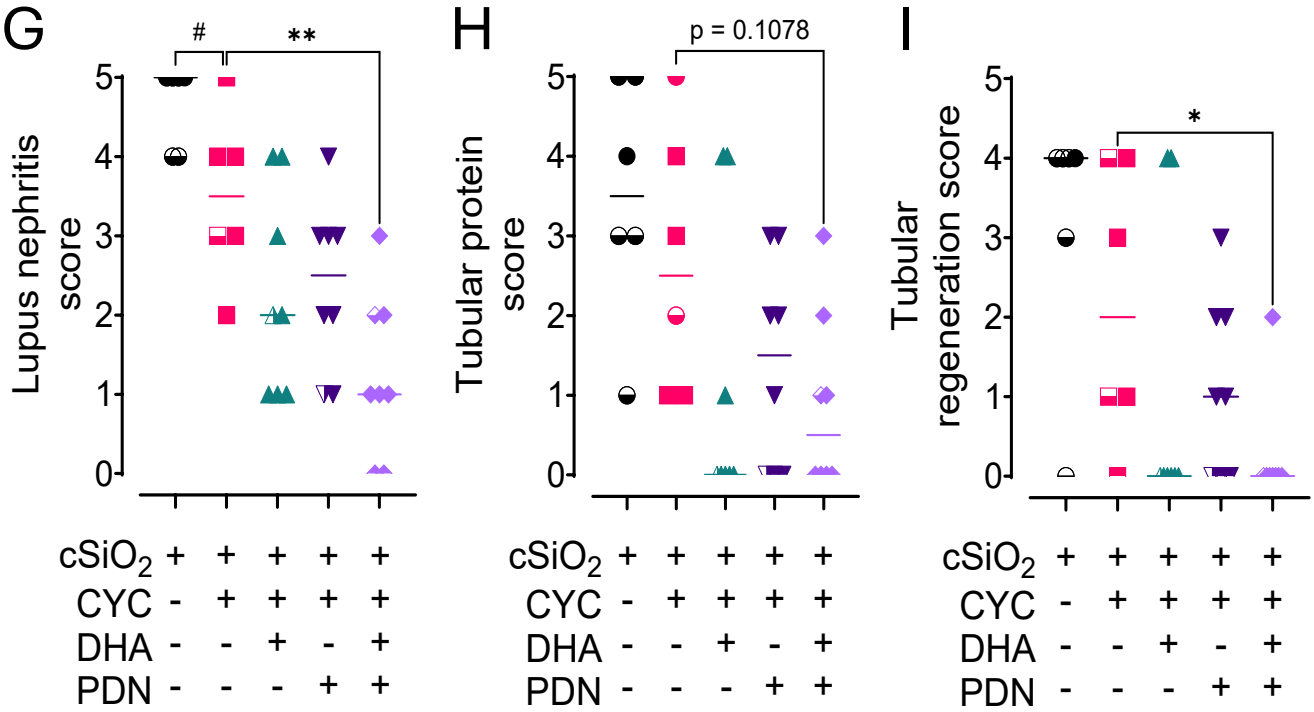
G
#
**
Lupus nephritis score
0
1
2
3
4
5
cSiO2 + + + + +
CYC - + + + +
DHA - - + - +
PDN - - - + +
H
p = 0.1078
Tubular protein score
0
1
2
3
4
5
cSiO2 + + + + +
CYC - + + + +
DHA - - + - +
PDN - - - + +
I
*
Tubular regeneration score
0
1
2
3
4
5
cSiO2 + + + + +
CYC - + + + +
DHA - - + - +
PDN - - - + +

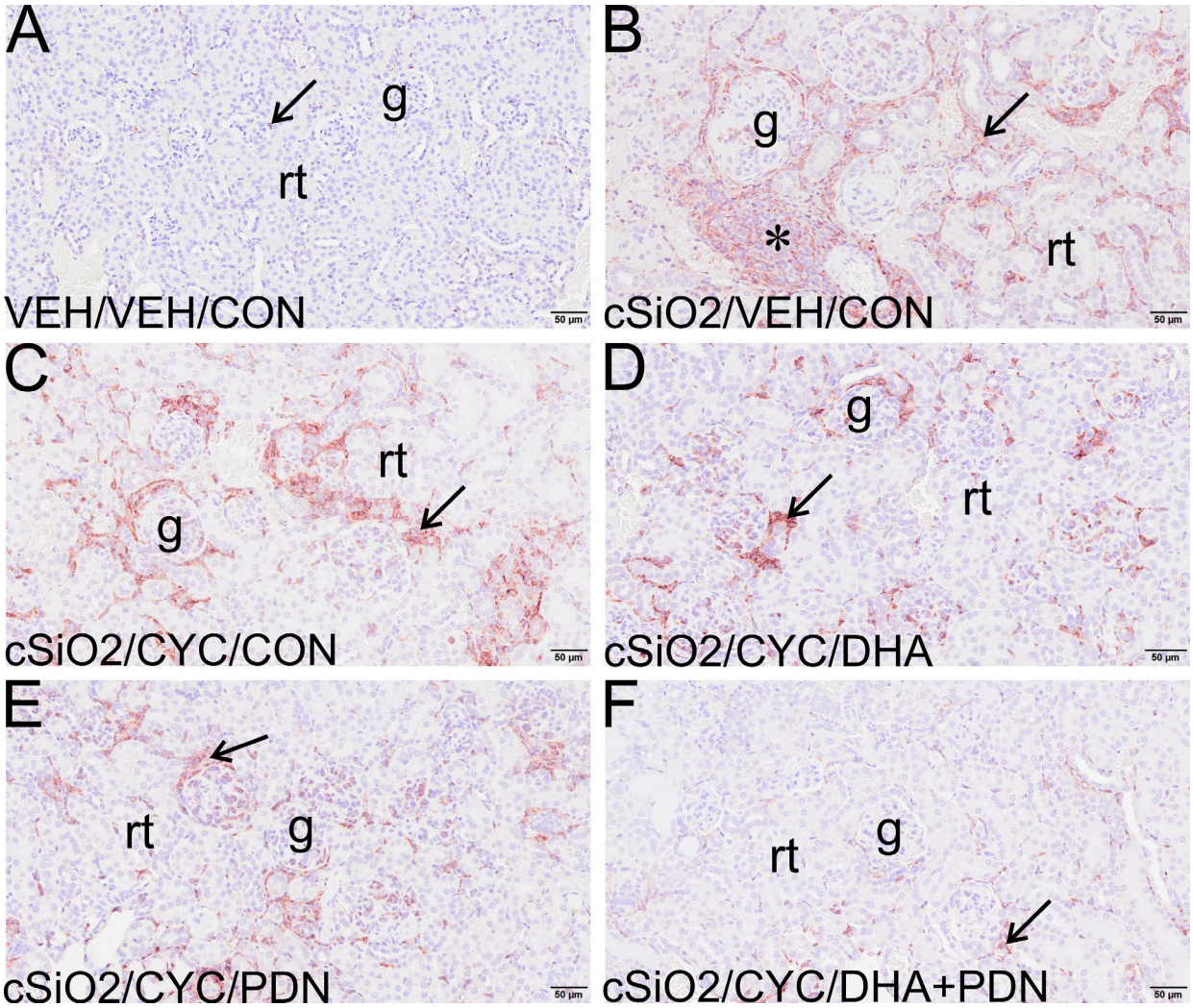
A
g
rt
VEH/VEH/CON
50 µm
B
g
*
rt
cSiO2/VEH/CON
50 µm
C
rt
g
cSiO2/CYC/CON
50 µm
D
g
rt
cSiO2/CYC/DHA
50 µm
E
rt
g
cSiO2/CYC/PDN
50 µm
F
rt
g
cSiO2/CYC/DHA+PDN
50 µm

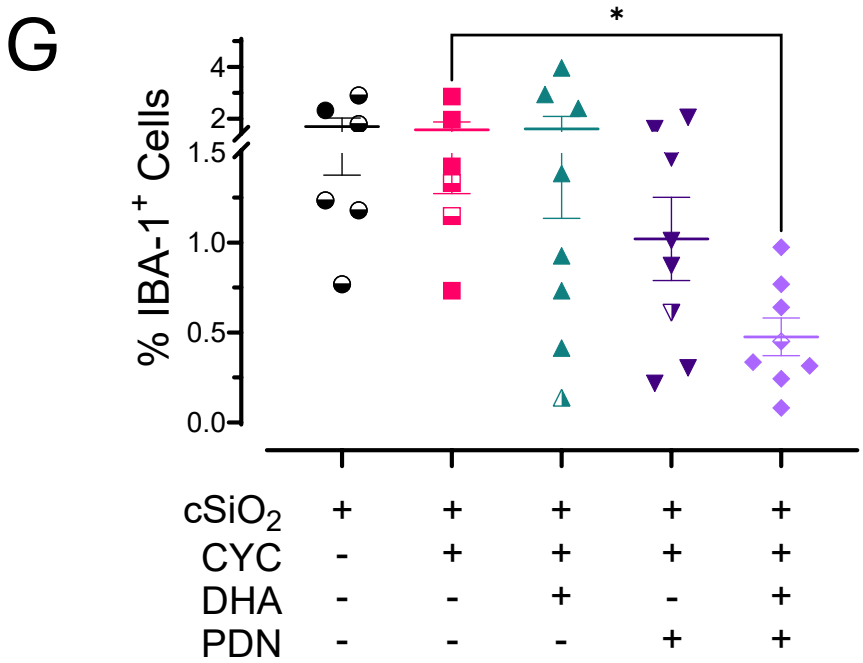
G
*
% IBA-1+ Cells
4
2
1.5
1.0
0.5
0.0
cSiO2 + + + + +
CYC - + + + +
DHA - - + - +
PDN - - - + +

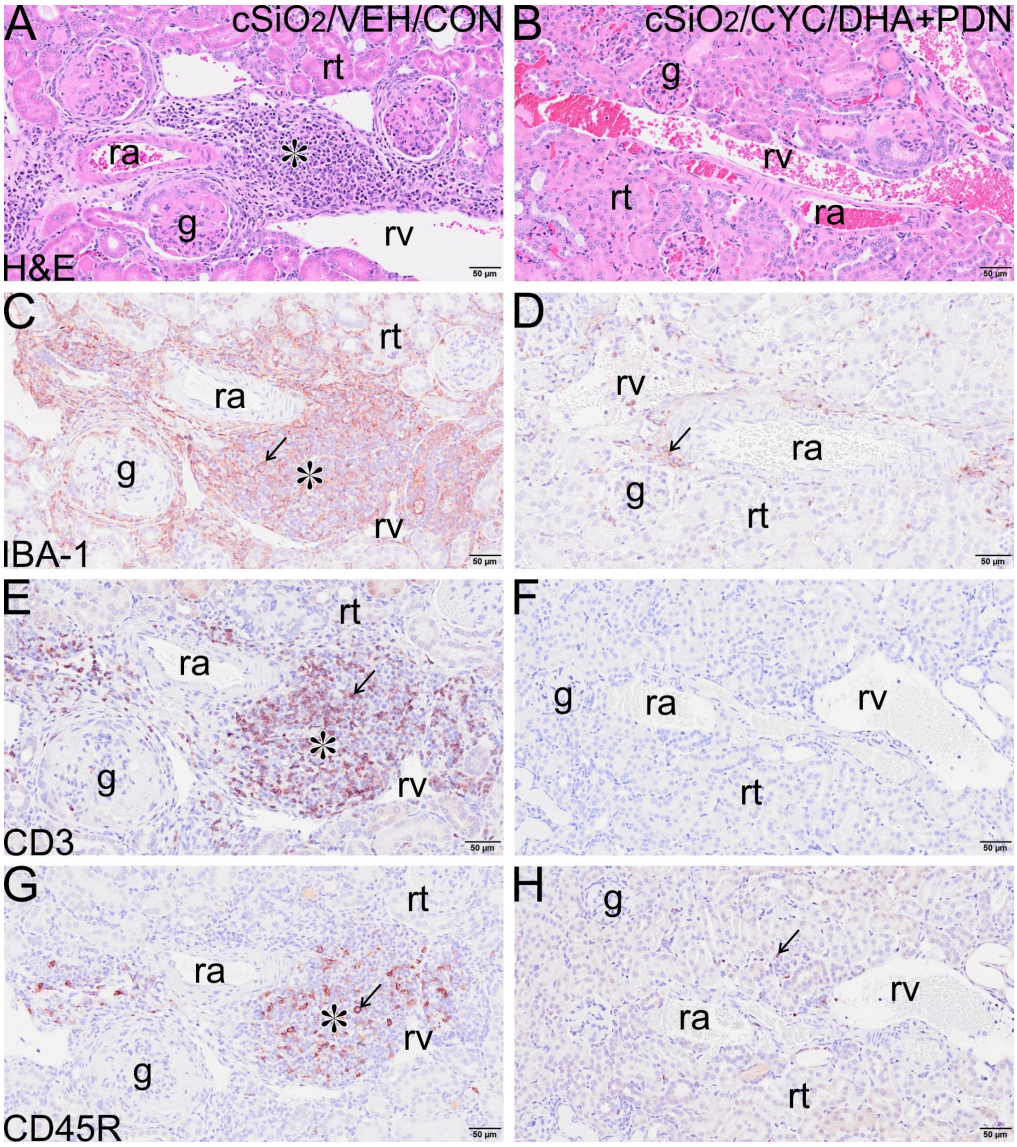
A
cSiO2/VEH/CON
rt
ra
g
rv
H&E
B
cSiO2/CYC/DHA+PDN
g
rv
rt
ra
C
rt
ra
g
rv
IBA-1
D
rv
ra
g
rt
E
rt
ra
g
rv
CD3
F
g
ra
rv
rt
G
rt
ra
g
rv
CD45R
H
g
rv
ra
rt

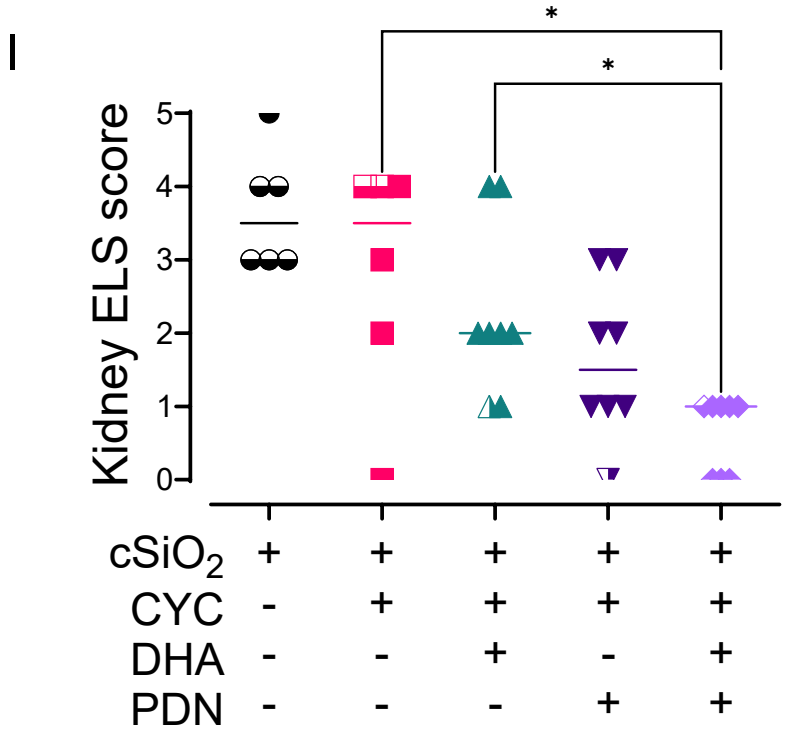
I
Kidney ELS score
0
1
2
3
4
5
*
*
cSiO2 + + + + +
CYC - + + + +
DHA - - + - +
PDN - - - + +

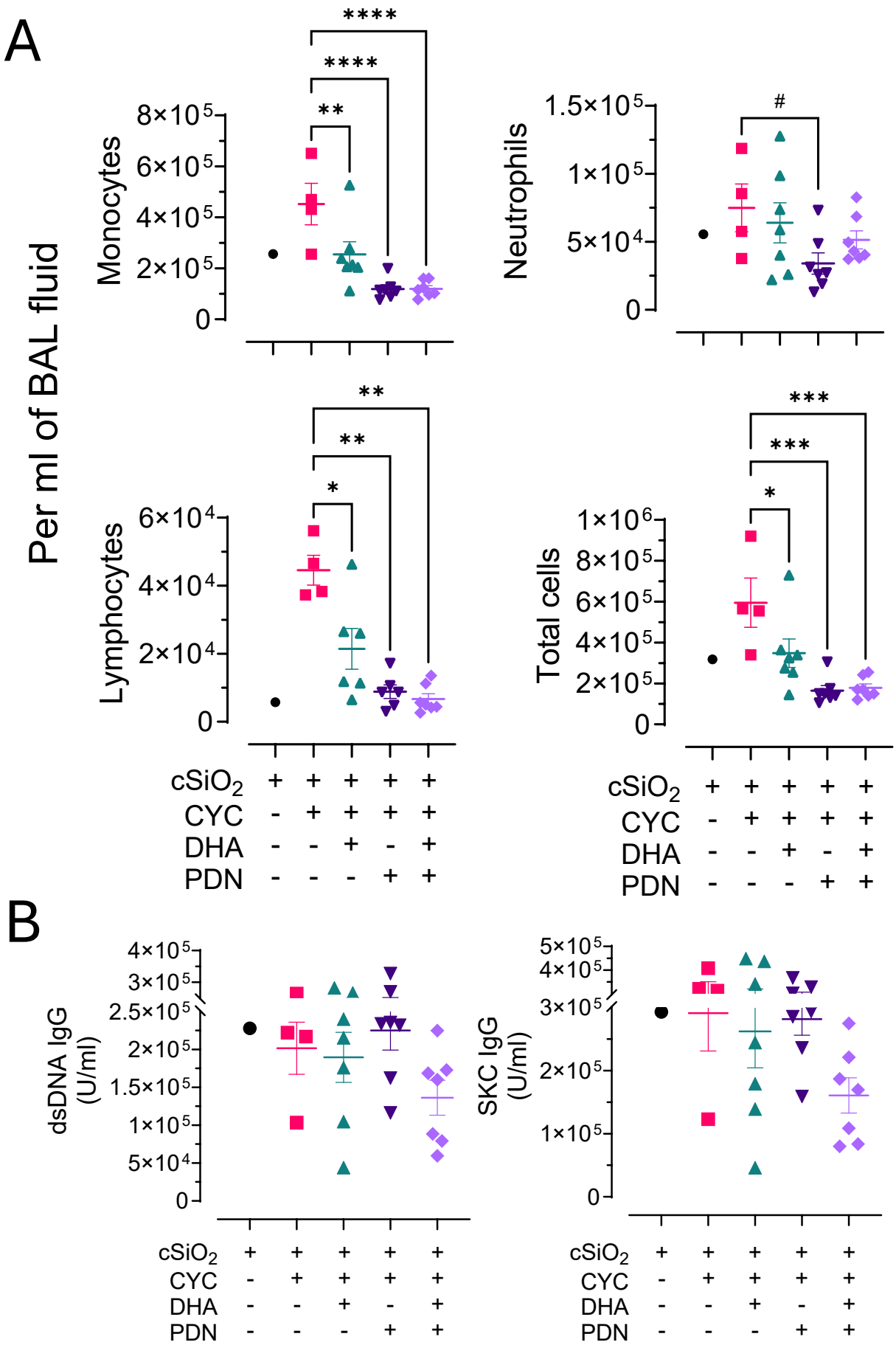
A
Per ml of BAL fluid
Monocytes
8×10^5
6×10^5
4×10^5
2×10^5
0
****
****
**
Neutrophils
1.5×10^5
1×10^5
5×10^4
0
#
Lymphocytes
6×10^4
4×10^4
2×10^4
0
**
**
*
Total cells
1×10^6
8×10^5
6×10^5
4×10^5
2×10^5
0
***
***
*
cSiO2 + + + + +
CYC - + + + +
DHA - - + - +
PDN - - - + +
B
dsDNA IgG (U/ml)
4×10^5
3×10^5
2.5×10^5
2×10^5
1.5×10^5
1×10^5
5×10^4
0
SKC IgG (U/ml)
5×10^5
4×10^5
3×10^5
2×10^5
1×10^5
0

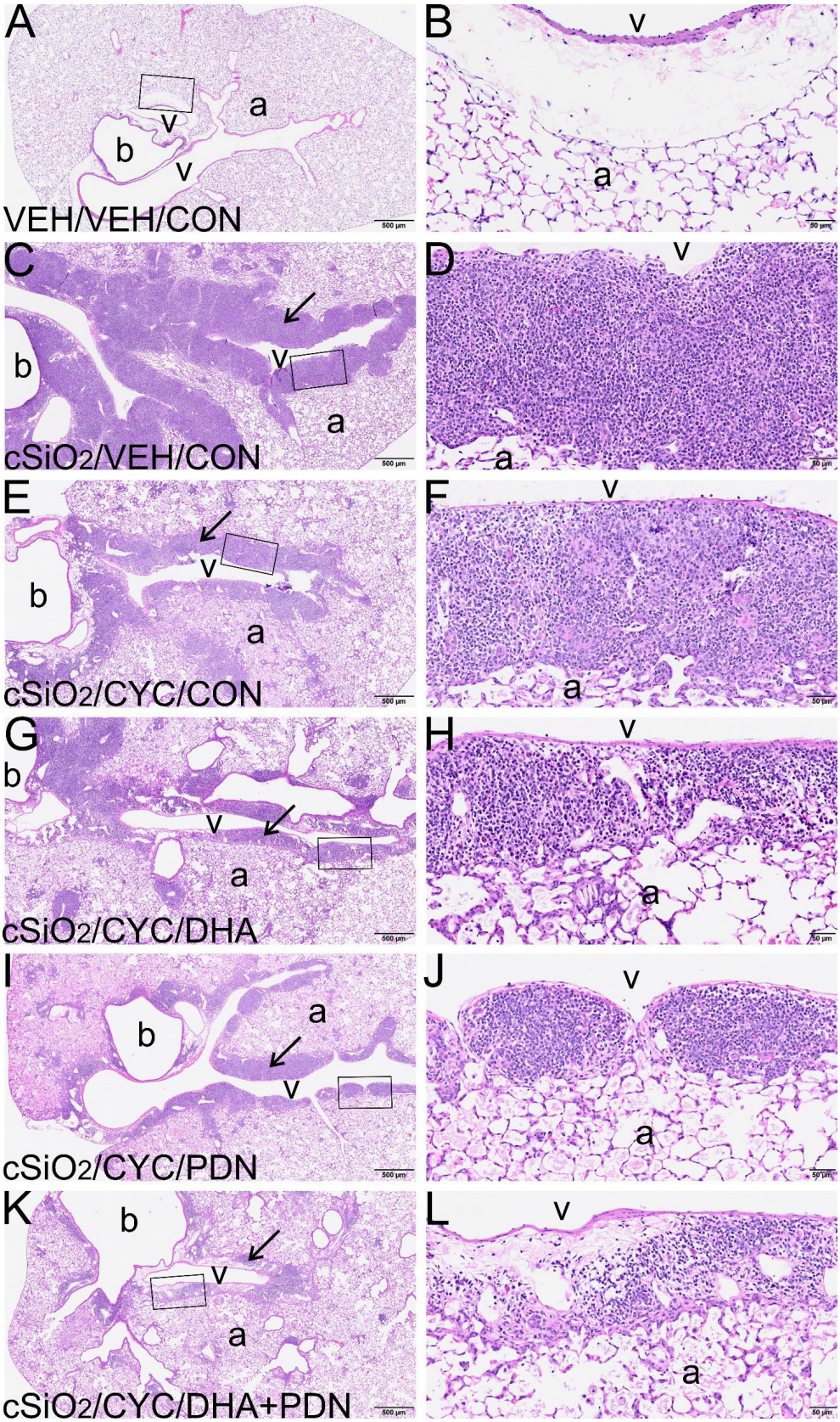
A
a
v
b
v
VEH/VEH/CON
B
v
a
C
b
v
a
cSiO2/VEH/CON
D
v
a
E
v
b
a
cSiO2/CYC/CON
F
v
a
G
b
v
a
cSiO2/CYC/DHA
H
v
a
I
b
a
v
cSiO2/CYC/PDN
J
v
a
K
b
v
a
cSiO2/CYC/DHA+PDN
L
v
a

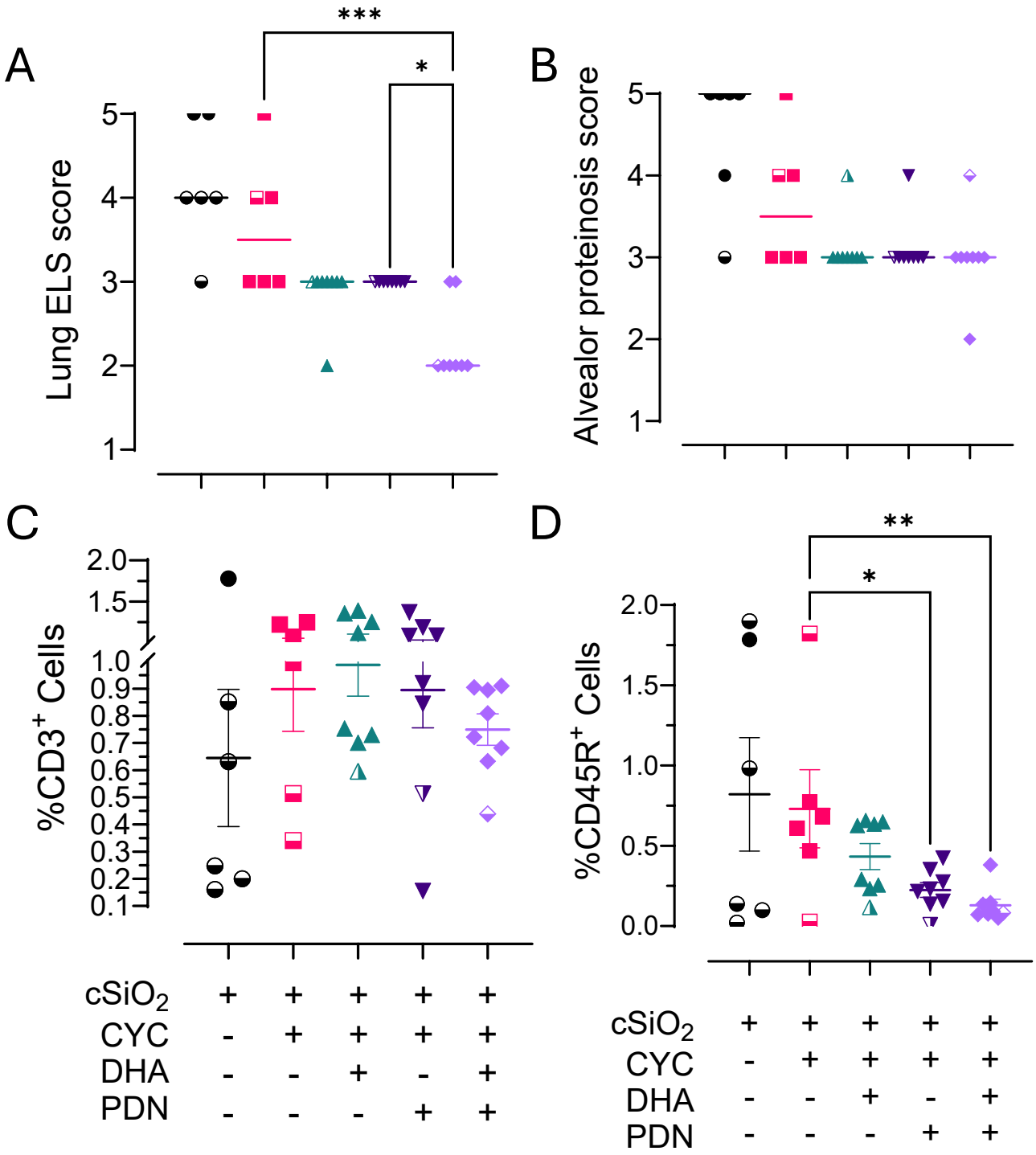
A
***
*
Lung ELS score
5
4
3
2
1
B
Alvealor proteinosis score
5
4
3
2
1
C
%CD3+ Cells
2.0
1.5
1.0
0.9
0.8
0.7
0.6
0.5
0.4
0.3
0.2
0.1
D
**
*
%CD45R+ Cells
2.0
1.5
1.0
0.5
0.0
cSiO2 + + + + +
CYC - + + + +
DHA - - + - +
PDN - - - + +
cSiO2 + + + + +
CYC - + + + +
DHA - - + - +
PDN - - - + +

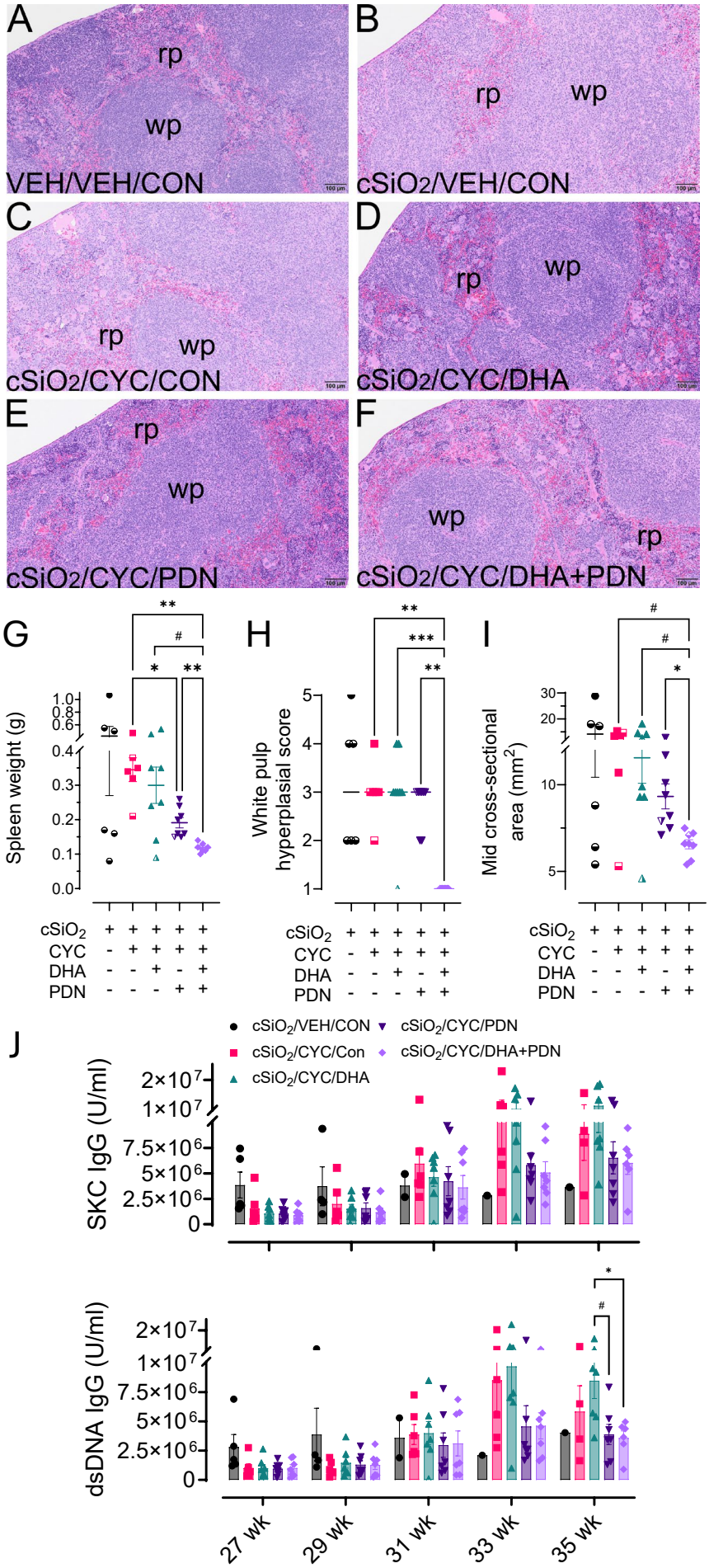
A
rp
wp
VEH/VEH/CON
B
rp
wp
cSiO2/VEH/CON
C
rp
wp
cSiO2/CYC/CON
D
rp
wp
cSiO2/CYC/DHA
E
rp
wp
cSiO2/CYC/PDN
F
wp
rp
cSiO2/CYC/DHA+PDN
G
Spleen weight (g)
H
White pulp hyperplasial score
I
Mid cross-sectional area (mm2)
cSiO2
CYC
DHA
PDN
J
cSiO2/VEH/CON
cSiO2/CYC/Con
cSiO2/CYC/DHA
cSiO2/CYC/PDN
cSiO2/CYC/DHA+PDN
SKC IgG (U/ml)
dsDNA IgG (U/ml)
27 wk
29 wk
31 wk
33 wk
35 wk

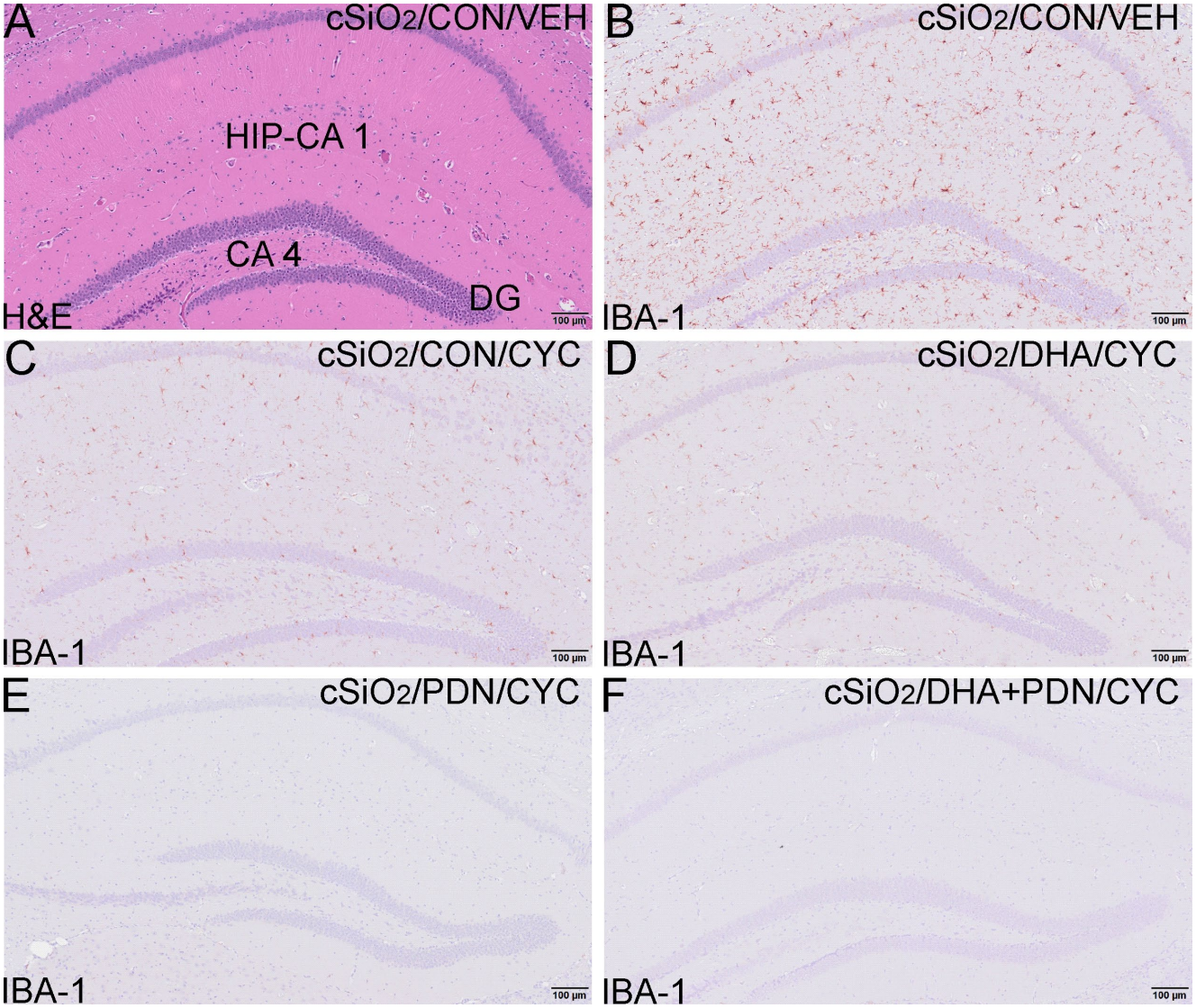
A
cSiO2/CON/VEH
HIP-CA 1
CA 4
DG
H&E
100 µm
B
cSiO2/CON/VEH
IBA-1
100 µm
C
cSiO2/CON/CYC
IBA-1
100 µm
D
cSiO2/DHA/CYC
IBA-1
100 µm
E
cSiO2/PDN/CYC
IBA-1
100 µm
F
cSiO2/DHA+PDN/CYC
IBA-1
100 µm

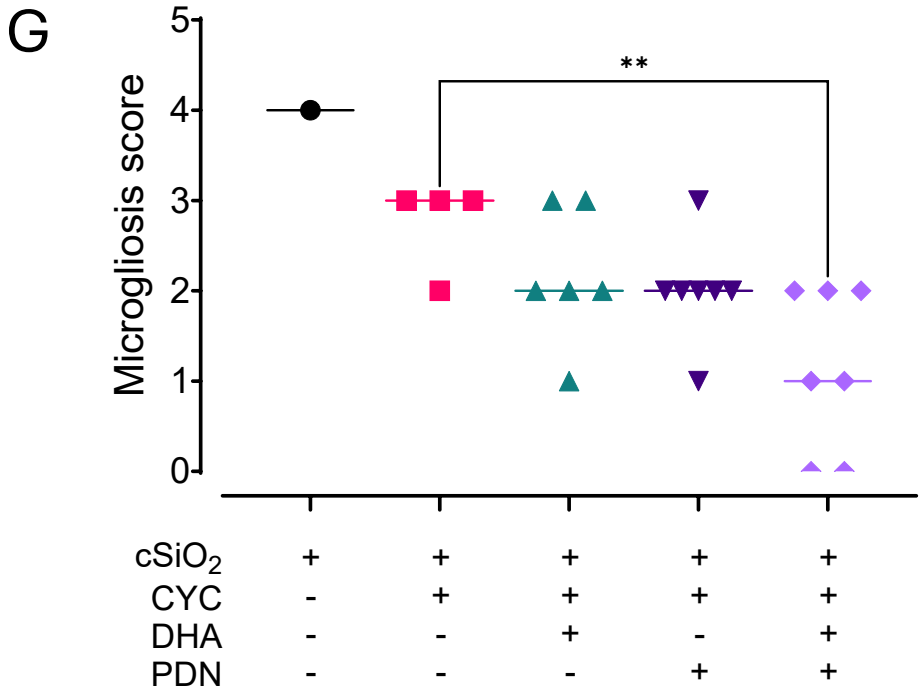
G
Microgliosis score
0
1
2
3
4
5
**
cSiO2 + + + + +
CYC - + + + +
DHA - - + - +
PDN - - - + +

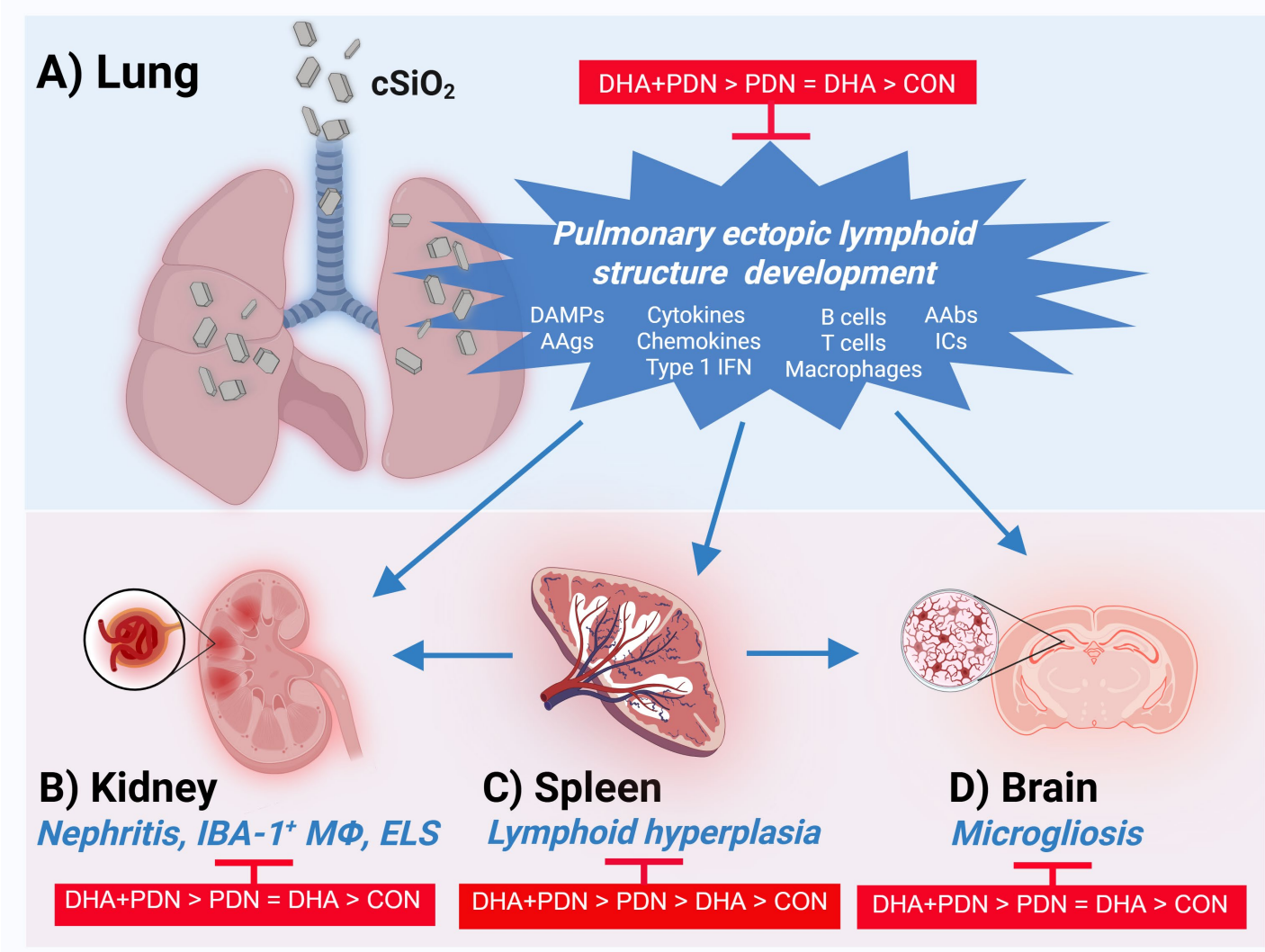
A) Lung
cSiO2
DHA+PDN > PDN = DHA > CON
Pulmonary ectopic lymphoid structure development
DAMPs
AAgs
Cytokines
Chemokines
Type 1 IFN
B cells
T cells
Macrophages
AAbs
ICs
B) Kidney
Nephritis, IBA-1+ MΦ, ELS
DHA+PDN > PDN = DHA > CON
C) Spleen
Lymphoid hyperplasia
DHA+PDN > PDN > DHA > CON
D) Brain
Microgliosis
DHA+PDN > PDN = DHA > CON

Reducing Glucocorticoid Burden in Lupus with Omega-3 Fatty Acids: Docosahexaenoic Acid Augments Prednisone Efficacy in Maintaining Cyclophosphamide-Induced Remission of Preclinical Lupus Nephritis

Ashley N. Anderson[1], Olivia F. McDonald[1,2], Shayla-Rae S. Johnson[1], John J. Liddle[1], Vanessa Estrada[1,2], Jalen T. Jackson[1], Ryan P. Lewandowski[3], James G. Wagner[2,3], Jack R. Harkema[2,3,4], James J. Pestka[1,2,5.]

[1]Department of Microbiology, Genetics, and Immunology, Michigan State University, East Lansing, MI, United States; [2]Institute for Integrative Toxicology, Michigan State University, East Lansing, MI, United States; [3]Department of Pathobiology and Diagnostic Investigation, Michigan State University, East Lansing, MI, United States; [4]Department of Pharmacology and Toxicology, Michigan State University, East Lansing, MI, United States; [5]Department of Food Science and Human Nutrition, Michigan State University, East Lansing, MI, United States

Supplemental Materials

- **Supplemental Methods:** Immunohistochemistry (IHC)
- **Supplementary Table 1.** List of key reagents, items, and kits
- **Supplementary Table 2.** Criteria for defining the moribund condition of silica-treated NZBWF1 mice
- **Supplemental Figure 1.** Effects of DHA and PDN monotherapies and co-therapy on CYC-induced reduction of blood urea nitrogen (BUN) in the $cSiO_2$-accelerated lupus nephritis mouse model

Supplemental Methods

Immunohistochemistry (IHC)

IHC was conducted as previously described (Pestka et al. 2021, Front. Immunol.12:653464). Briefly, formalin-fixed, paraffin-embedded samples were sectioned, placed on charged slides, and dried overnight at 56°C. The slides were then deparaffinized in xylene and rehydrated using a dilution series of ethanol ending with distilled water. Slides were immersed in tris-buffered saline pH 7.4 (TBS, Scytek Labs, Logan, UT) for 5 minutes to adjust the pH. Following TBS, retrieval protocols were applied according to the requirements of each primary antibody. Endogenous peroxidase activity was blocked for 30 minutes at room temperature in a solution of 3% hydrogen peroxide in methanol (1:4), then rinsed with running tap water, followed by several rinses in distilled water, and a 5-minute incubation in TBS containing Tween 20 (Scytek Labs, Logan, UT). After pretreatment, standard micropolymer complex staining steps were performed at room temperature using the Biocare Medical intelliPATH FLX automated IHC staining instrument. Rinses after each staining step were carried out with TBS autowash buffer containing surfactant (TWB945M, Biocare Medical, Pacheco, CA).

After blocking for nonspecific protein with rodent block M (Biocare Medical, Pacheco, CA) or IntelliPATH background punisher (IP974G20, Biocare Medical, Pacheco, CA) for 20 or 5 minutes, respectively, tissue sections were incubated with primary antibodies (anti-IBA-1, 1:3,000, anti-CD3 1:200, anti-CD45R 1:250) in normal antibody diluent (Scytek Labs, Logan, UT). MicroPolymer Rabbit on Rodent HRP Polymer was used for the CD3 and IBA-1 primary antibodies, and Rat on Mouse HRP Probe and Polymer were used for the CD45R primary antibody. To visualize the target proteins, the substrate Biocare Medical Romulin AEC Chromogen was incubated with the tissue for 5 minutes, then counterstained with CATHE Hematoxylin (Biocare Medical, Pacheco, CA) at a dilution of 1:10 for 1 minute. Afterwards, slides were air-dried, cleared, and mounted with synthetic mounting media.

Supplementary Table 1. List of key reagents, items, and kits.

Reagent, item, or kit	Vendor	Catalog Number
AIN-93G Purified Rodent Diet without Vitamin Mix	Dyets Inc.	110700
AIN-93VX Vitamin Mix	Dyets Inc.	310025
LouAna Safflower Oil	LouAna Oils	
AVO high-oleic safflower oil	American Vegetable Oils, Inc.	
Mazola Corn Oil	Mazola	
Cyclophosphamide	Sigma-Aldrich	C0768-1G
Prednisone	Spectrum Chemical Mfg. Corp.	PR103-25GM
DHASCO, Microalgal Oil Containing 40% DHA	DSM Nutritional Products	
Crystalline Silica	U.S. Silica	Min-U-Sil-5
Polyclonal Rabbit Anti – IBA-1	Wako Fuji	019-19741
Polyclonal Rabbit anti – CD3	Abcam	ab5690
Monoclonal Rat anti – Mouse CD45R	BD Pharmingen	550286
Uristix 4	Siemens Healthineers	
CLINITEK Status+ Urine Analyzer	Siemens Healthineers	
Urea Nitrogen (BUN) Detection Assay Kit (Colorimetric)	RayBiotech	MA-BUN-5
Mouse Cytokine/Chemokine 44-Plex Discovery Assay® Array	Eve Technologies	MD44
Nunc 96-Well Flat Bottom MaxiSorp Immuno Plates	Thermo Fisher Scientific	442404
Corning® Phosphate-Buffered Saline, 1X without calcium and magnesium, PH 7.4 ± 0.1	Corning	21-040-CV
HyClone DPBS 10X without calcium, magnesium	Cytiva	SH30378.03
Poly-L-Lysine Solution, 0.1% (w/v)	Sigma Aldrich	P8920
Purified Native dsDNA, Calf Thymus	Alpha Diagnostic International	DNAD25-N-1
Anti-DNA Antibody, double stranded, clone BV16-13	Millipore Sigma	MAB030
Goat Anti-Mouse IgG (heavy-chain sp.)-HRP conjugate	Alpha Diagnostic International	40120
K-Blue® Advanced TMB Substrate	Neogen	319176

Supplementary Table 2. Criteria for defining moribund condition of silica-treated NZBWF1 mice[a]

Criteria	Method	Response	Score Assigned
Proteinuria[1,2]	Weekly monitoring	<2000 mg/dl = negative (NEG)	0
		>2000 mg/dl = positive (POS)	1
	Note: proteinuria scoring is cumulative over time		
	e.g., POS for proteinuria at 22 wks of age and POS at 23 wks of age = cumulative score of 2		
Weight Loss[2,3,4,5]	Weekly body weight	<10% loss = NEG	0
		10-14% loss = POS	2
		>15% loss = POS	4
	Note #1: loss of body weight will be calculated relative to body weight at onset of nephritis		
	Note #2: onset of nephritis defined as = 300 mg/dl proteinuria (determined in above measurements)		
Dyspenia[1,3,4,5,*]	Daily health check	Qualitative - NO	0
		Qualitative - YES	1
Ambulation[3,4,5,*]	Daily health check	Qualitative - NO	0
		Qualitative - YES	4
Rough Coat[3,4,5,*]	Daily health check	Qualitative - NO	0
		Qualitative - YES	1

[a] Table was reviewed by CAR Veterinarian Dr. Danielle Ferguson at Michigan State University. Mice receiving a score of 4 or more were euthanized. References for criteria previously published indicated by superscripts and noted below.

[1]Gardet et al. (2016) PLOS ONE. 11(10): e 0164423
[2]Frese-Schaper et al. (2010) J Immunology 184 (4) 2175-2182
[3]Toth, L. (2000). Journal of the Institute for Laboratory Animal Research (2000) 41 (2): 72-29
[4]Toth, L. (1997). Contemp. Top Lab Anim Sci 36, 44-48
[5]Tomasovic et al. (1988). Lab Animal 17:31-34,1998.
*The IACUC Handbook (2014) CRC Press. 3rd Edition

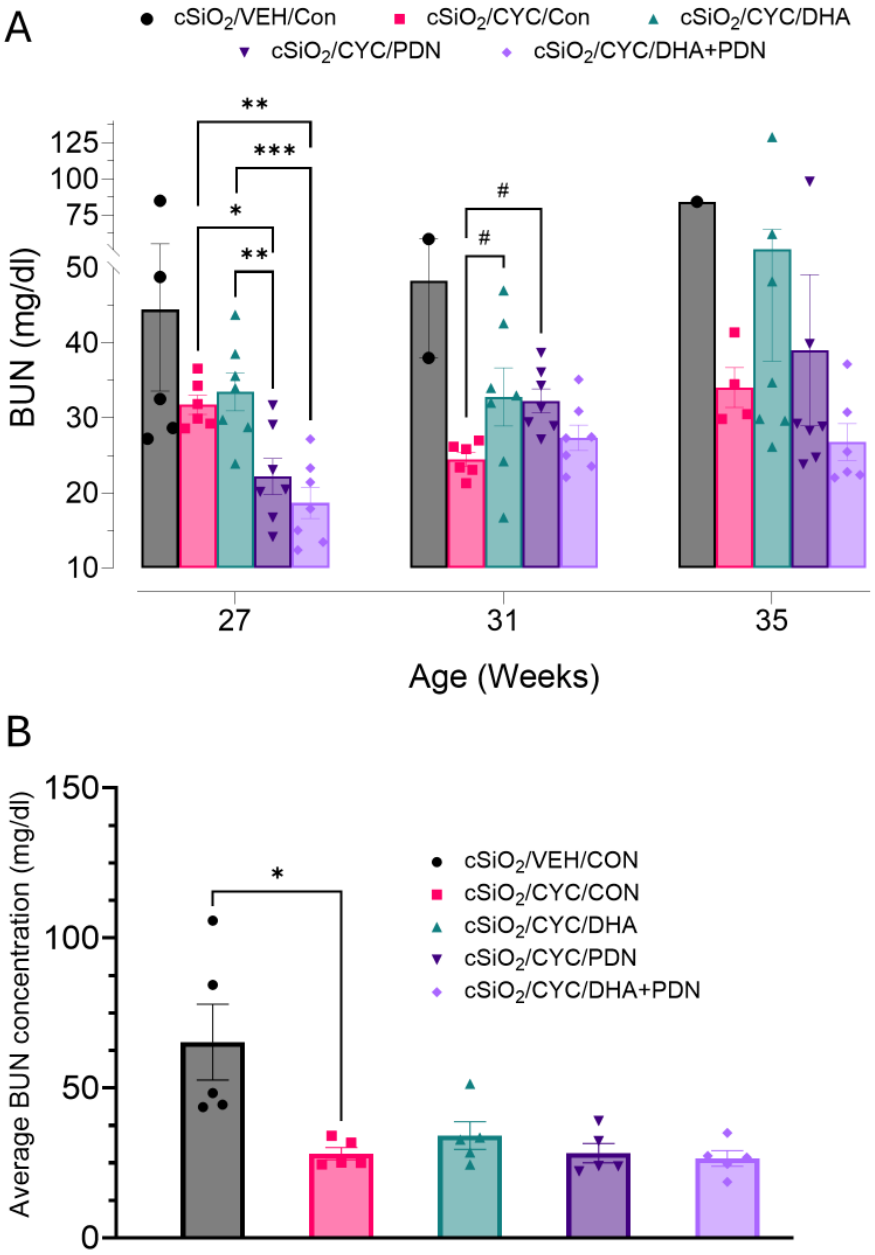

Supplemental Figure 1. Effects of DHA and PDN monotherapies and co-therapy on CYC-induced reduction of blood urea nitrogen (BUN) in the $cSiO_2$-accelerated lupus nephritis mouse model. (A) BUN values at specific time points during the study. (B) Average BUN levels from weeks 27-35 of the study. Symbols: #, *, **, and *** denote significant differences at the $p<0.1$, $p<0.05$, $p<0.01$, and $p<0.001$ levels, respectively.